Original article

Sulphonamido-quinoxalines: Search for anticancer agent

CrossMark

Rahul Ingle [a], Rajendra Marathe [b], Dipak Magar [c], Harun M. Patel [a,*], Sanjay J. Surana [a]

[a] Department of Pharmaceutical Chemistry, R.C. Patel College of Pharmacy, Shirpur, Dhule 425405, Maharashtra, India
[b] Department of Pharmaceutical Chemistry, Government College of Pharmacy, Amravati 424605, Maharashtra, India
[c] Department of Pharmaceutical Chemistry, Dr. Bhanuben Nanawati College of Pharmacy, Mumbai 400056, Maharashtra, India

ARTICLE INFO

Dedicated to my late mother Ms. Ajija Patel, who was the source of inspiration for me.

ABSTRACT

A series of new sulphonamido-quinoxaline derivatives 3(a–p) have been prepared which are structurally similar to the High Throughput Screening (HTS) hit identified by Porter and collaborator. The newly synthesized compounds 3b, 3c, 3f, 3i, 3j, 3l, 3n and 3o were further evaluated in the National Cancer Institute for in vitro cytotoxicity assay among them compound 3l showed highest activity against Leukemia RPMI-8226 cell lines (GI_{50}: 1.11 μM) as compared to other tested compounds. It is to be noted that compound 3l shows significant activity (GI_{50}: 1.11 μM) compared to the High Throughput Screening (HTS) hit identified by Porter and collaborator ($IC_{50} = 1.3$ μM). Further docking study confirms the c-Met kinase inhibitory mechanism of the synthesized compounds.

© 2013 Elsevier Masson SAS. All rights reserved.

1. Introduction

Members of the receptor tyrosine kinase (RTK) family are attractive targets for cancer therapy as inhibition can disrupt signaling pathways that mediate tumor formation and growth [1–3]. c-Met kinase is a member of this family that, together with its ligand, hepatocyte growth factor (HGF) or scatter factor (SF), is important for normal mammalian development. However, c-Met has been shown to be deregulated and associated with high tumor grade and poor prognosis in a number of human cancers [4,5]. c-Met can become activated by a variety of mechanisms, including gene amplification and mutation inducing motility, invasiveness and tumourgenicity into the transformed cells [6–10]. Activation leads to receptor dimerization and recruitment of several SH2 domain containing signal transducers that activate a number of pathways including the Raf-Mek-Erk and PI3k-Akt cascades [9,11–14]. Targeting the ATP binding site of c-Met is a popular strategy for inhibition of the kinase, many small molecules selectively targeting the ATP binding site of c-Met kinase have been identified and exerted significant therapeutic effects in treating human cancers clinically [9,12,13,15,16]. Quinoxalines and quinoxalinones are attractive chemical candidates in medicinal chemistry due to their capacity to generate biological responses in their interaction with several biological targets. They show antiviral [15], herbicidal [16] and anti-inflammatory action [17]. Recent investigations revealed the pharmacological potential of quinoxalines as anticancer agents [18] and numerous theoretical studies were performed on quinoxaline and its derivatives, in order to find new antineoplastic compounds.

Porter and collaborator recent investigation pointed out the quinoxaline scaffold as a template to the design of inhibitors of c-Met kinase [19]. In the course of one high throughput screening campaign, they selected one quinoxaline derivative as the most promising structure to inhibit selectively the ATP binding site of c-Met ($IC_{50} = 1.3$ μM in the c-Met biochemical assay) [19]. After that, they successfully optimized the activity of the original structure by preparing and testing a set of quinoxalines. Following Porter's research, we decided to contribute in the analysis of the interaction of quinoxalines with c-Met kinase.

Hence in continuation of our efforts on the design and synthesis of novel anticancer agents [20–25] and keeping in mind the medicinal importance of quinoxaline moiety, in the present study we synthesized and in vitro evaluated quinoxalines at National Cancer Institute (NCI-USA) for antitumor activity. We have also tried to dock the synthesized compounds with the crystal structure of c-Met kinase (PDB: 2wgj) to explore the possible anticancer mechanism of our compounds and similarly further analyzed the synthesized compounds for Lipinski's rule of five to

* Corresponding author. Tel.: +91 8806621544; fax: +91 1881263655.
E-mail address: hpatel_38@yahoo.com (H.M. Patel).

evaluate drug likeness and established in silico ADME parameters using QikProp.

2. Rationale and designing

In this study, we present a new sub-family of compounds containing 2,3,6-trisubstituted quinoxalines as c-Met kinase inhibitors. We have designed the ligands which are structurally similar to the High Throughput Screening (HTS) hit identified by Porter and collaborator as shown in Figs. 1–4 [19]. Porter and collaborator suggested that for the better activity quinoxaline should have basic nitrogen substituent; they also suggested that replacement of the amino methyl linker by sulfonamide group increases the activity; hence we put sulphonamido (−SO₂NH−) substituents at 6th position of quinoxaline. Further wide range of substituted phenyl analogs were prepared by them, suggesting that such bulky group

accommodate into the hydrophobic pocket of c-Met kinase; therefore we introduced phenyl ring at 2nd and 3rd position of quinoxaline to increase hydrophobic interaction with receptor c-Met kinase [19].

On the other hand PF-2341066 (crizotinib) has been identified as an ATP-competitive c-Met inhibitor [13,26]. We analyzed the crizotinib structure deposited in PDB (PDBcode: 2wgj) and identified that the 2-aminopyridine (crizotinib) bound to the hinge region of c-Met and interact with the amidal NH of Met-1160 via nitrogen of pyridine forming hydrogen-bonding interaction. Furthermore, we found that 2,6-di-chloro-3-fluorophenyl ring formed a hydrophobic interaction with c-Met kinase (Fig. 3), these hydrophobic interactions may contribute to the selective inhibition of c-Met kinase.

While exploring the scaffold of c-Met selective inhibitor, we hypothesized that the hydrophobic interactions were essential and the binding affinity enhanced by adding the hydrophobic space filler
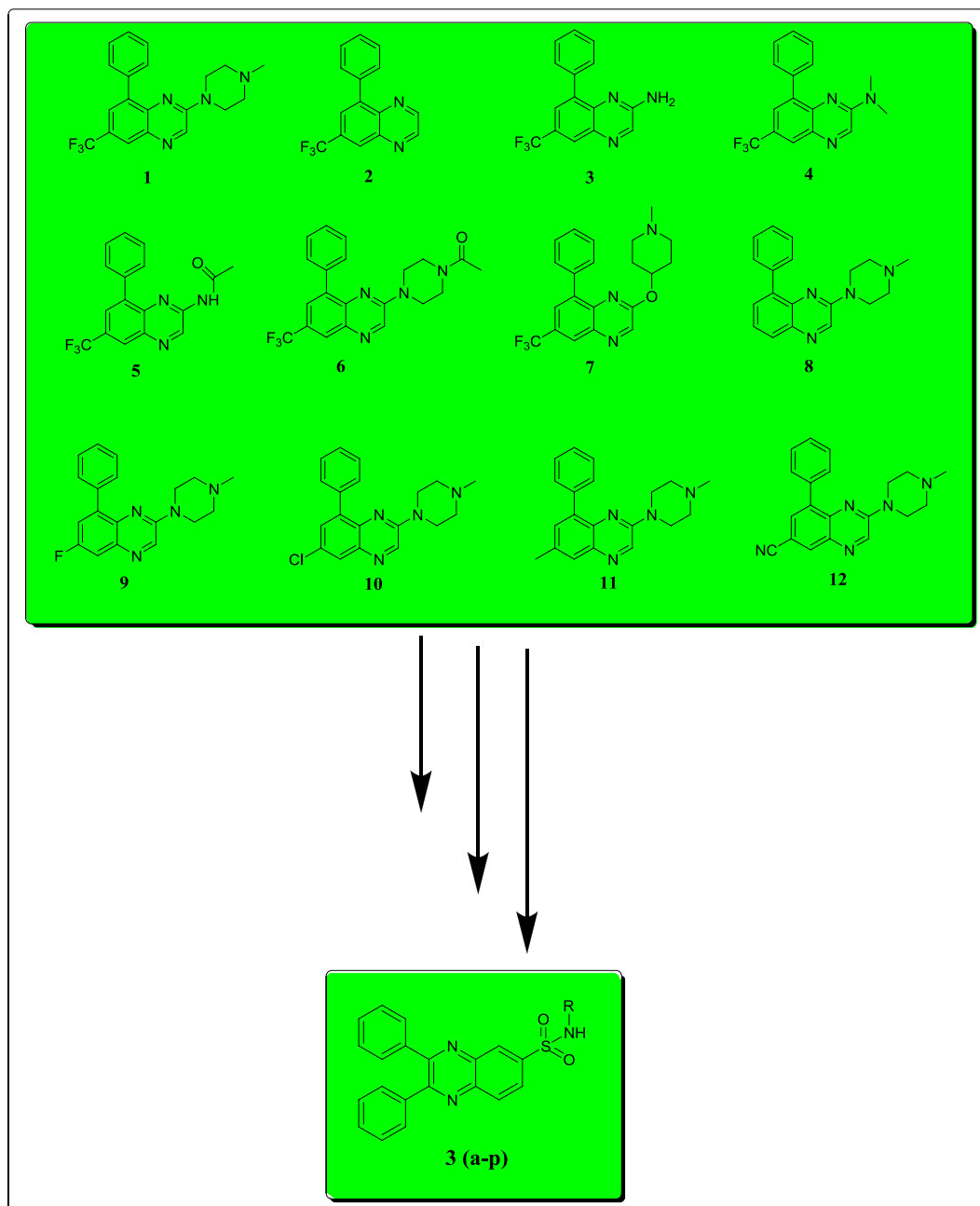

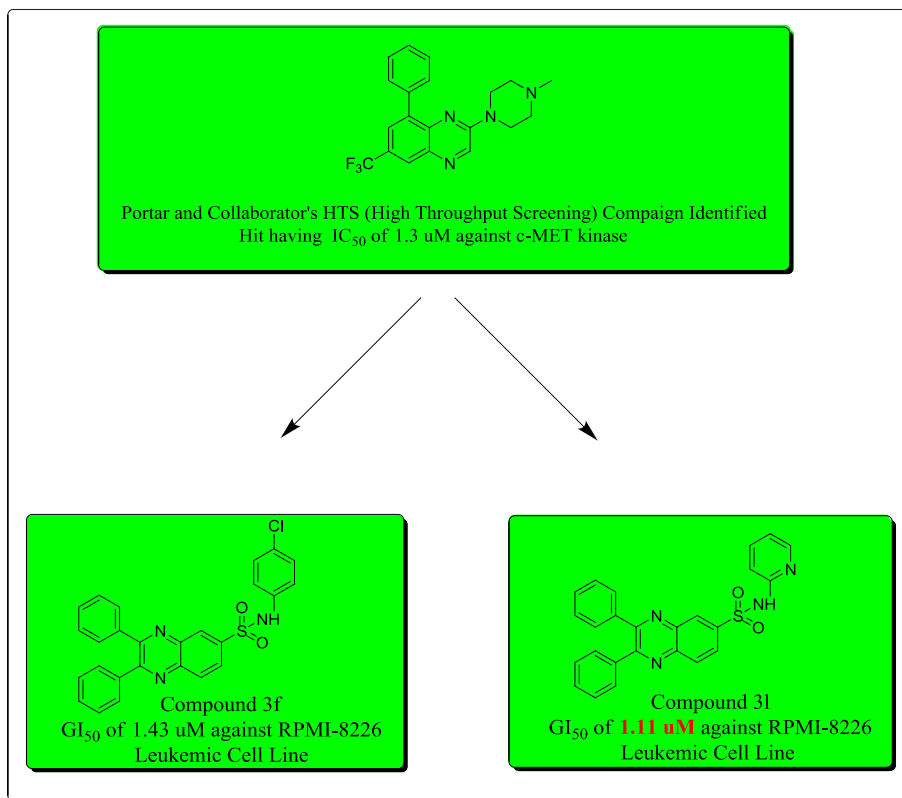**Fig. 1.** Reported and proposed antitumor quinoxaline derivatives.

Fig. 2. Rationale designing of the proposed compounds based upon High Throughput Screening (HTS) hit identified by Porter and collaborator.

with the core structure as shown in Fig. 3. Based on these hypotheses, we designed core structure containing 6-sulphonamido quinoxaline as the scaffold to form the three interactions: (1) the hydrogen bond with the hinge region (Met-1160), (2) bulky moiety at 6th position of the quinoxalines in a fashion similar to crizotinib which binds in the ATP-binding cleft, so that the bulky group could be oriented deep in the back of the ATP binding site and makes predominantly hydrophobic interactions with the protein mimicking the 2,6-di-chloro-3-fluorophenyl group of crizotinib, (3) hydrophobic space-filling with a quinoxaline skeleton as shown in Fig. 3.

3. Results and discussion

3.1. Chemistry

The synthesis of compounds **3**(**a**–**p**) is given in Scheme 1. The present study includes synthesis of sulphonyl chloride derivatives of 2,3-diphenylquinoxaline **2** by addition–elimination reaction mechanism. 2,3-Diphenylquinoxaline **1** was treated with chlorosulfonic acid under ice cold condition to give 6-sulfonyl chloride-2,3-diphenylquinoxaline **2** [27]. It was further refluxed with the different amines by using 10% aq. NaOH to yield sulphonyl chloride derivatives of quinoxaline **3**(**a**–**p**) by nucleophilic substitution reaction. Physical data of the synthesized compounds **3**(**a**–**p**) is shown in Table 1.

The derivatives were characterized by spectral studies using IR, ^{1}H NMR, ^{13}C NMR and HRMS. The structures of 2,3-diphenylquinoxaline-6-sulfonyl chloride **2** was confirmed by the IR absorption peak at $\sim$1350, 1150 cm^{-1} (S=O) and $\sim$700 cm^{-1} corresponding to Cl. N-Substituted-2,3-diphenylquinoxaline-6-

sulfonamide **3**(**a**–**p**) were confirmed by the absence of characteristic IR absorption peak at $\sim$700 cm^{-1} of Cl and presence of NH stretch bands at $\sim$3300 cm^{-1}; further occurrence of broad singlet peak at $\sim\delta$ 5 ppm corresponding –NH group in ^{1}H NMR substantiated the formation of sulphonamido-quinoxalines **3**(**a**–**p**). ^{13}C NMR and HRMS gave information about carbon atoms and all the M$^+$ ion peaks corresponding to molecular weight of confirmed novel compounds.

3.2. Pharmacology

3.2.1. Primary single high dose (10^{-5} M) full NCI 60 cell panel in vitro assay

All the synthesized compounds **3**(**a**–**p**) were submitted to the National Cancer Institute (NCI, Bethesda, MD) for the human tumor cell screen. Among them eight compounds **3b** (NSC: 763437), **3c** (NSC: 763438), **3f** (NSC: 763442), **3i** (NSC: 763441), **3j** (NSC: 763440), **3l** (NSC: 763439), **3n** (NSC: 763435) and **3o** (NSC: 763436) were selected and tested initially at a single high dose (10 μM concentration) in the full NCI 60 cell panel as shown in Table 2. Effective one-dose assay has been added to the NCI 60 cell screen in order to increase compound throughput and reduce data turnaround time to suppliers while maintaining efficient identification of active compounds. All the selected compounds were tested initially at a single high dose in the full NCI 60 cell panel including leukemia, non-small cell lung, colon, CNS, melanoma, ovarian, renal, prostate and breast cancer cell lines. Only compounds which satisfy pre-determined threshold inhibition criteria would progress to the five-dose screen. The threshold inhibition criterion for progression to the five-dose screen were designed to efficiently capture compounds with anti-proliferative activity and is based on
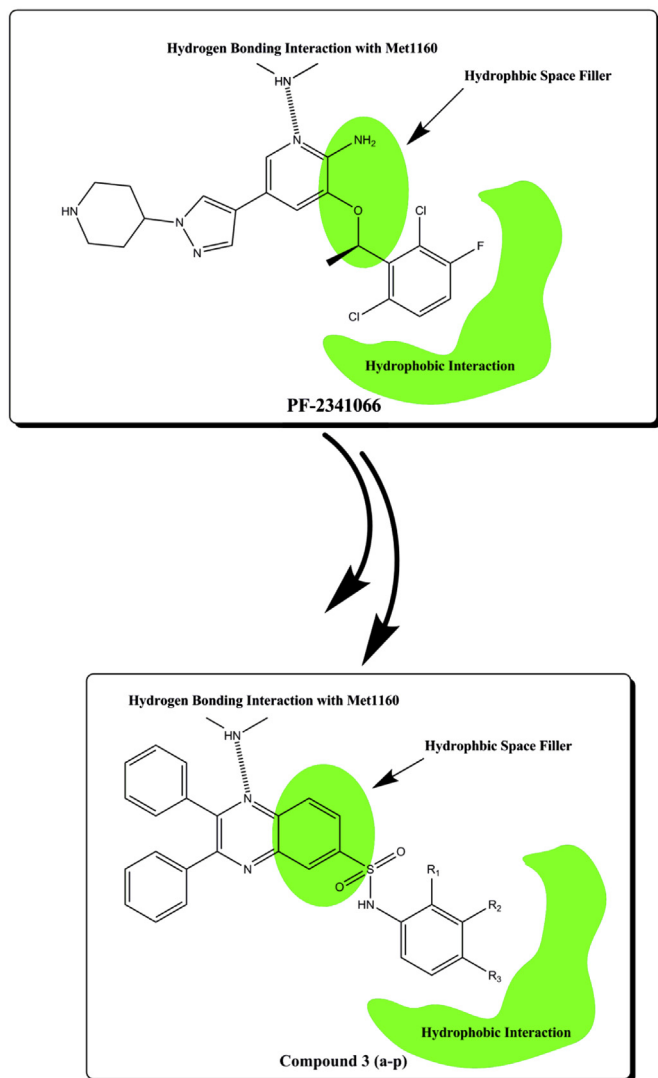
Fig. 3. Proposed hypothetical model of the highly active PF-2341066 (crizotinib)/c-Met cocrystal structure and quinoxaline **3**(**a**–**p**) bound to c-Met kinase.

careful analysis of historical Development Therapeutic Program (DTP) screening data. The data are reported as a mean-graph of the percent growth of treated cells, and presented as percentage growth inhibition (GI%) caused by the test compounds. The obtained results showed that out of eight compounds **3f** (NSC: 763442) and **3l** (NSC: 763439) passed successfully this primary anticancer assay and were consequently carried over to the five-dose screen against a panel of about 60 different tumor cell lines. For each compound in the 5-dose screen, anticancer activity was deduced from dose–response curves and expressed by three parameters (GI$_{50}$, TGI, LC$_{50}$) calculated for each cell line. The GI$_{50}$ value indicates the concentration of the compound required to cause 50% inhibition of net cell growth. The TGI value represents the concentration of the compound resulting in total inhibition of net cell growth. The LC$_{50}$ value refers to the concentration of the compound leading to 50% net cell death [28–30].

3.2.2. In vitro 5 dose full NCI 60 cell panel assay

All the cell lines (about 60), representing nine tumor subpanels, were incubated at five different concentrations (0.01, 0.1, 1, 10 & 100 μM). The outcomes were used to create log concentration Vs%

growth inhibition curves and three response parameters (GI$_{50}$, TGI and LC$_{50}$) were calculated for each cell line. The GI$_{50}$ value (growth inhibitory activity) corresponds to the concentration of the compound causing 50% decrease in net cell growth, the TGI value (cytostatic activity) is the concentration of the compound resulting in total growth inhibition and LC$_{50}$ value (cytotoxic activity) is the concentration of the compound causing net 50% loss of initial cells at the end of the incubation period of 48 h [28–30].

Compound **3f** (NSC: 763442) exhibited high activity against Leukemia HL-60 (GI$_{50}$: 2.09 μM) and RPMI-8226 cell lines (GI$_{50}$: 1.43 μM); Non Small Cell Lung Cancer HOP-62 (GI$_{50}$: 3.95 μM) and HOP-92 cell line (GI$_{50}$: 2.03 μM); CNS Cancer SNB-75 cell line (GI$_{50}$: 2.12 μM); Prostate Cancer PC-3 cell line (GI$_{50}$: 1.47 μM) and Breast T-47D Cancer cell line (GI$_{50}$: 1.62 μM) as shown in Figs. 5 and 6. Similarly compound under investigation **3l** (NSC: 763439) exhibited significant anticancer activity against most of the tested cell lines representing nine different subpanels with GI$_{50}$ values between 1.11 to 4.54 μM and found to be potential candidate of the series as shown in Figs. 7 and 8. With regard to the sensitivity against some individual cell lines the compound **3l** showed highest activity against Leukemia RPMI-8226 cell lines (GI$_{50}$: 1.11 μM) and least against Non Small Cell Lung Cancer HOP-62 cell line (GI$_{50}$: 4.54 μM). It is to be noted that compound **3l** shows significant activity (GI$_{50}$: 1.11 μM) as compared to the High Throughput Screening (HTS) hit identified by Porter and collaborator with IC$_{50}$ = 1.3 μM [19]. Toxicity is measured in terms of lethality; both compounds are not lethal and safe in nature as it is obvious by examining the LC$_{50}$ value as shown in Figs. 5 and 7.

3.2.3. Structure activity relationship

The various sulphonamido-quinoxaline derivatives **3**(**a**–**p**) have been synthesized in the present study and subjected to in vitro anticancer activity assay at National Cancer Institute. The results were summarized in Table 2 and Figs. 5 and 7. Structure activity correlation, in terms of NCI selected compounds (**3b**, **3c**, **3f**, **3i**, **3j**, **3l**, **3n** and **3o**), based on the number of cell lines proved sensitive toward each of the synthesized individual compounds, revealed that, the quinoxaline ring is a satisfactory backbone for antitumor activity. The presence of substituted amino moiety at the C-6 position is necessary for the activity as hydrophobic region. The presence of electron withdrawing group on substituted amino moiety at 6th position enhances the anticancer activity it is obvious by comparing anticancer results of compound **3f** with **3b**, **3c**, **3i**, **3j**, **3n** and **3o**. Sulphonamido (–SO$_2$NH–) group at 6th position of quinoxaline is acting as conformational lock and extending the bulky group into the hydrophobic pockets of c-Met kinase, making predominantly hydrophobic interactions with the protein mimicking the 2,6-dichloro-3-fluorophenyl group of crizotinib as it is obvious from docking study. If we compare the anticancer results of five dose selected compounds **3f** (GI$_{50}$ 1.43 μM against RPMI-8226 Leukemic cell line) and **3l** (GI$_{50}$ 1.11 μM against RPMI-8226 Leukemic cell line); it is seen that **3l** is showing significant anticancer activity as compared to **3f** as shown in Figs. 5 and 7; here once again it is proved that for better activity quinoxaline should have basic nitrogen substituent at 6th position.

3.3. Docking study and drug likeliness

The molecular docking tool, GLIDE (Schordinger Inc., USA) was used for ligand docking studies into c-Met kinase receptor binding pocket. The crystal structure of c-Met kinase was obtained from protein data bank (PDB: 2wgj) [28]. The protein preparation was carried out using 'protein preparation wizard' in Maestro 9.0 in two steps, preparation and refinement. After ensuring chemical correctness, water molecules in the crystal structures were deleted
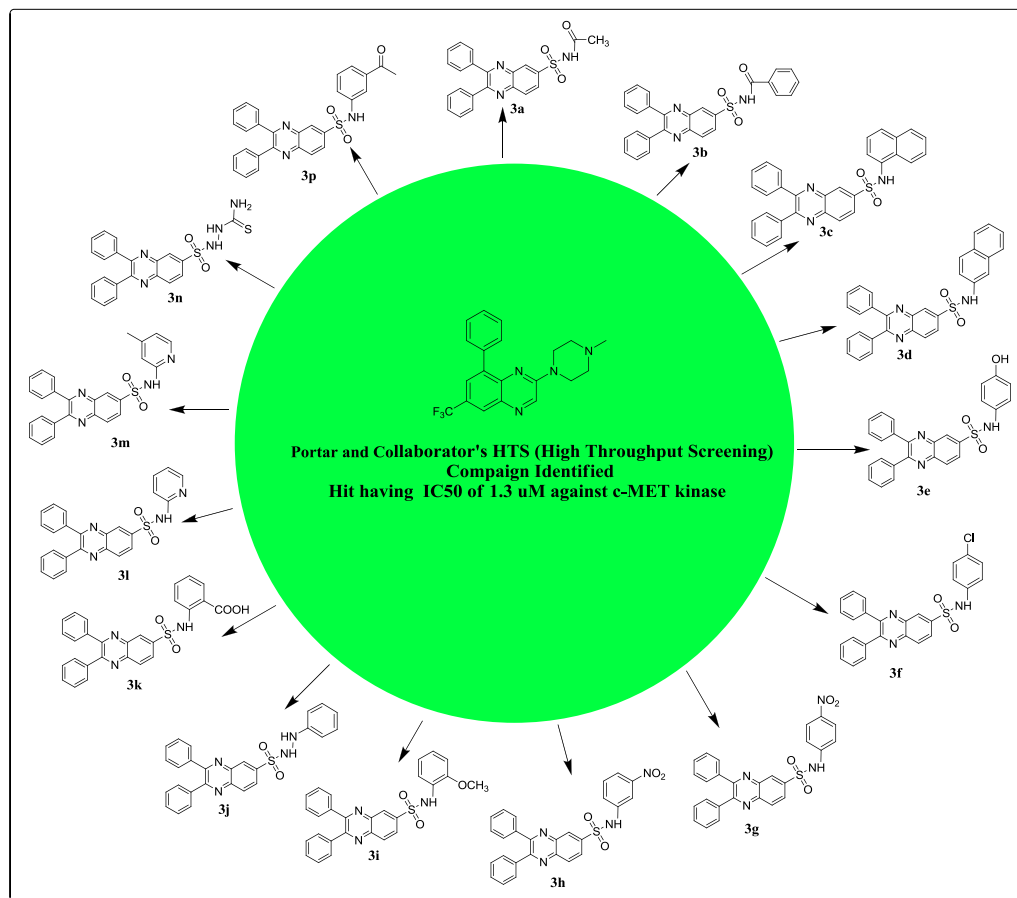
Fig. 4. Sulphonamido-quinoxalines **3**(**a**–**p**) rationally designed by High Throughput Screening (HTS) hit identified by Porter and collaborator.
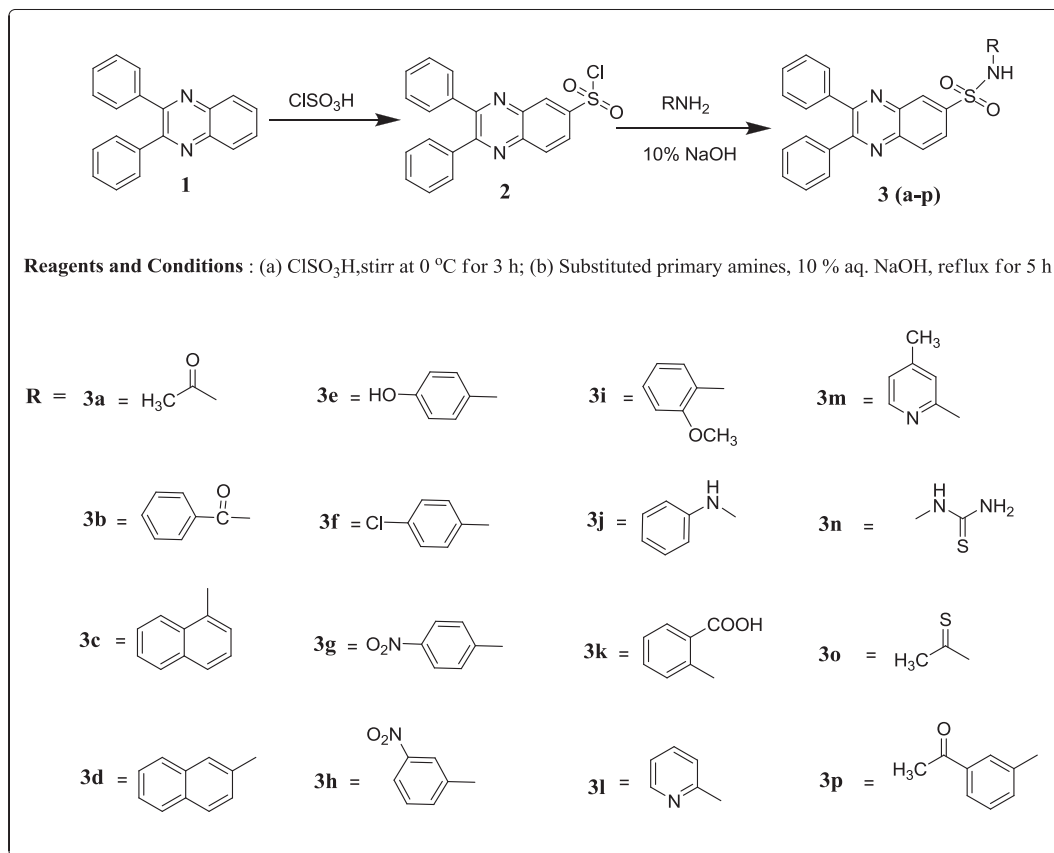
and hydrogens were added, where they were missing. Using the OPLS 2005 force field energy of crystal structure was minimized [29]. Grids were defined centering them on the ligand in the crystal structure using the default box size. The ligands were built using maestro build panel and prepared by Ligprep 2.2 module which produce the low energy conformer of ligands using OPLS 2005 force field. The low energy conformation of the ligands was selected and was docked into the grid generated from protein structures using standard precision (SP) docking mode. The final evaluation is done with glide score (docking score) and single best pose is generated as the output for particular ligand.

Since it was found that crizotinib mimic ATP and bind to the ATP binding region of the kinase active site. Our compounds were modeled by positioning them in the crizotinib binding site. From the comparative docking study of our compounds with structurally related lead compound such as crizotinib we could observe how our compounds might bind to the kinase binding site, based on the knowledge of the structure of similar active sites. We redocked crizotinib into the active site of the enzyme and then we replaced with our compounds in order to compare the binding mode of both ligand and the test compound. These docking studies have revealed that the quinoxaline ring binds to a narrow hydrophobic pocket in the domain of c-Met kinase where N-4 of the quinoxaline ring interacts with the backbone NH of Met-1160 via a hydrogen bond (Table 1 and Fig. 9). These interactions underscore the importance of both nitrogen atoms for binding and the subsequent inhibitory capacity. Similarly SO_2NH_2 group at 6th position also shows additional two hydrogen bonding interaction (S=O with Tyr-1159 and NH with Lys-1161). Among the docked compounds **3**(**a**–**p**),

compound **3p**, **3f** and **3l** shows the highest docking score of −8.6538, −8.2164 and −8.5808 respectively, the detail is given in Table 1. Highest docking score of compound **3p** shows that it could be having significant anticancer activity as compared to the compound **3f** and **3l** but it is not selected at NCI-USA for the anticancer screening. The results of this virtual screening could support the postulation that our active compounds may act on the same enzyme target c-Met kinase. It is also seen that bulky moiety at 6th position of the quinoxaline in a fashion similar to crizotinib oriented deep in the back of the ATP binding site and makes predominantly hydrophobic interactions with the protein mimicking the 2,6-di-chloro-3-fluorophenyl group of crizotinib.

Fig. 9 demonstrate binding mode of crizotinib and quinoxaline derivatives **3f** and **3l**. Crizotinib forms hydrogen bonding with Met-1160 via N-1 of pyridine ring and similar hydrogen bonding interaction is also shown by N-4 of quinoxaline (**3f** and **3l**) with Met-1160. Residues within 5 Å areas of crizotinib and quinoxaline derivatives **3f** and **3l** are shown in Fig. 9. Some common residues involved in this type of interaction within 5 Å area are VAL-1092, TYR-1159, ALA-1108, MET-1211, ARG-1208, ILE-1084, and ASP-1231.

We further analyzed physically significant descriptors and pharmaceutically relevant properties of all synthesized compounds, among which were molecular weight, LogP, H-bond donors, H-bond acceptors according to Lipinski's rule of five (Table 3). Lipinski's rule of five is a rule of thumb to evaluate drug likeness, or determine if a chemical compound with a certain pharmacological or biological activity has properties that would make it a likely orally active drug in humans. The rule describes delicate balance among the molecular properties of a

Reagents and Conditions : (a) ClSO₃H,stirr at 0 °C for 3 h; (b) Substituted primary amines, 10 % aq. NaOH, reflux for 5 h

Scheme 1. Reaction scheme for the synthesis of target compounds **3**(**a**–**p**).

compound that directly influence its pharmacodynamics and pharmacokinetics and ultimately affect their absorption, distribution, metabolism, and excretion in human body like a drug [30]. In general, these parameters allow to ascertain a poor oral absorption, or membrane permeability, that occurs when the evaluated molecules present values higher than five H-bond donors (HBD), 10 H-bond acceptors (HBA), molecular weight (MW) > 500 Da and LogP (cLogP) > 5 (Lipinski's 'rule-of-five') [31]. The compounds were evaluated for their drug-like behavior through analysis of pharmacokinetic parameters required for absorption, distribution, metabolism and excretion (ADME) by use of QikProp [32].

For the 16 compounds, the partition co-efficient (QPlogPo/w) and water solubility (QPlogS), critical for estimation of absorption and distribution of drugs within the body ranged between 2.591 to 5.39 and −6.788 to −4.897. Cell permeability (QPPCaco), a key factor governing drug metabolism and its access to biological membranes, ranged from 40.588 to 981.419, QPPMDCK ranges from 19.782 to 1085.791. Overall, the percentage human oral absorption for the compounds ranged from 81.389 to 100%. All these pharmacokinetic parameters are within the acceptable range defined for human use (see Table 3 footnote), thereby indicating their potential as drug-like molecules.

4. Conclusion

In conclusion a new series of sulphonamido-quinoxalines **3**(**a**–**p**) were synthesized. Among all of these derivatives, compounds **3b** (NSC: 763437), **3c** (NSC: 763438), **3f** (NSC: 763442), **3i** (NSC: 763441), **3j** (NSC: 763440), **3l** (NSC: 763439), **3n** (NSC: 763435) and **3o** (NSC: 763436) were tested at a single dose of 10^{-5} M concentration at the NCI over 60 cell line panel, and compounds **3f** and **3l** were subsequently tested in 5-dose testing mode. With regard to the sensitivity against some individual cell lines the compound **3l** showed highest activity against Leukemia RPMI-8226 cell lines (GI₅₀: 1.11 μM) as compared to other tested compounds. It is to be noted that compound **3l** shows significant activity (GI₅₀: 1.11 μM) as compared to the High Throughput Screening (HTS) hit identified by Porter and collaborator with IC₅₀ = 1.3 μM. Molecular docking studies further supports our assumption that the synthesized compounds have analogous binding mode to the c-Met kinase inhibitors and demonstrates the various interactions between the ligands and enzyme active sites and thereby help to design novel potent inhibitors. The overall outcome of this model revealed that: (i) the quinoxaline ring is a satisfactory backbone for antitumor activity; (ii) the presence of substituted amino moiety at the C-6 position is necessary for the activity as hydrophobic region; (iii) the presence of electron withdrawing group on substituted amino moiety at 6th position enhances the anticancer activity; (iv) sulphonamido (−SO₂NH−) group at 6th position of quinoxaline is acting as conformational lock and extending the bulky group into the hydrophobic pockets of c-Met kinase, making predominantly hydrophobic interactions with the protein mimicking the 2,6-dichloro-3-fluorophenyl group of crizotinib. Lipinski's rule and in silico ADME pharmacokinetic parameters are within the acceptable range defined for human use thereby indicating their potential as drug-like molecules. These encouraging results of biological screening of the tested compounds could offer an excellent framework in this field that may lead to discovery of potent antitumor agent. Finally it is conceivable that further derivatization of such compounds will be of interest with the hope to get more selective anticancer agents.

Table 1

Physicochemical properties of the synthesized compounds **3**(**a**–**p**) and glide docking results based on glide dock score, glide energy, glide pose and hydrogen bonding interaction.
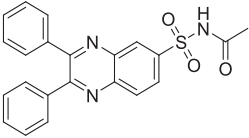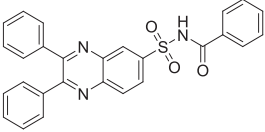
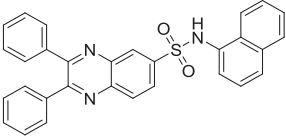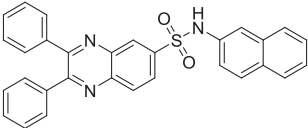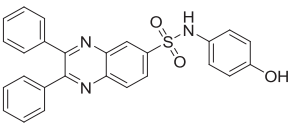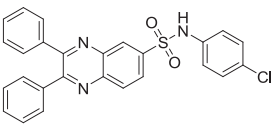| S. no.	Compounds	Molecular formula	Melting point (°C)	Percentage yield (%)	Docking score	Glide energy (kcal/mol)	Glide pose	H-bond interaction
3a		$C_{22}H_{17}N_3O_3S$	146–150	72	−5.7239	−43.3463	220	N- of quinoxaline and H atom of amino acid backbone of MET-1160 S=O of sulphonamido with H atom of amino acid Tyr-1159 NH of sulphonamido with carbonyl oxygen of Lys-1161
3b		$C_{27}H_{19}N_3O_3S$	172–176	68	−4.9109	−42.7556	284	N- of quinoxaline and H atom of amino acid backbone of MET-1160 S=O of sulphonamido with H atom of amino acid Tyr-1159 NH of sulphonamido with carbonyl oxygen of Lys-1161
3c		$C_{30}H_{21}N_3O_2S$	182–186	53	−7.9830	−48.4402	393	N- of quinoxaline and H atom of amino acid backbone of MET-1160 S=O of sulphonamido with H atom of amino acid Tyr-1159 NH of sulphonamido with carbonyl oxygen of Lys-1161
3d		$C_{30}H_{21}N_3O_2S$	190–194	58	−5.7691	−57.1301	176	N- of quinoxaline and H atom of amino acid backbone of MET-1160 S=O of sulphonamido with H atom of amino acid Tyr-1159 NH of sulphonamido with carbonyl oxygen of Lys-1161
3e		$C_{26}H_{19}N_3O_3S$	202–204	56	−7.0208	−54.8931	45	N- of quinoxaline and H atom of amino acid backbone of MET-1160 S=O of sulphonamido with H atom of amino acid Tyr-1159 NH of sulphonamido with carbonyl oxygen of Lys-1161
3f		$C_{26}H_{18}ClN_3O_2S$	222–226	74	−8.5808	−50.0947	295	N- of quinoxaline and H atom of amino acid backbone of MET-1160 S=O of sulphonamido with H atom of amino acid Tyr-1159 NH of sulphonamido with carbonyl oxygen of Lys-1161

Table 1 (*continued*)

S. no.	Compounds	Molecular formula	Melting point (°C)	Percentage yield (%)	Docking score	Glide energy (kcal/mol)	Glide pose	H-bond interaction
3g		$C_{26}H_{18}N_4O_4S$	178–182	79	−7.4131	−58.8267	384	N- of quinoxaline and H atom of amino acid backbone of MET-1160 S=O of sulphonamido with H atom of amino acid Tyr-1159 NH of sulphonamido with carbonyl oxygen of Lys-1161
3h		$C_{26}H_{18}N_4O_4S$	192–196	69	−7.3535	−58.8077	56	N- of quinoxaline and H atom of amino acid backbone of MET-1160 S=O of sulphonamido with H atom of amino acid Tyr-1159 NH of sulphonamido with carbonyl oxygen of Lys-1161
3i		$C_{27}H_{21}N_3O_3S$	202–204	59	−6.4248	−50.2353	94	N- of quinoxaline and H atom of amino acid backbone of MET-1160 S=O of sulphonamido with H atom of amino acid Tyr-1159 NH of sulphonamido with carbonyl oxygen of Lys-1161
3j		$C_{26}H_{20}N_4O_2S$	208–212	68	−6.1365	−49.0306	242	N- of quinoxaline and H atom of amino acid backbone of MET-1160 S=O of sulphonamido with H atom of amino acid Tyr-1159 NH of sulphonamido with carbonyl oxygen of Lys-1161
3k		$C_{27}H_{19}N_3O_4S$	234–238	71	−6.0096	−47.4862	150	N- of quinoxaline and H atom of amino acid backbone of MET-1160 S=O of sulphonamido with H atom of amino acid Tyr-1159 NH of sulphonamido with carbonyl oxygen of Lys-1161
3l		$C_{25}H_{18}N_4O_2S$	246–250	74	−8.2164	−50.1261	232	N- of quinoxaline and H atom of amino acid backbone of MET-1160 S=O of sulphonamido with H atom of amino acid Tyr-1159 NH of sulphonamido with carbonyl oxygen of Lys-1161
3m		$C_{26}H_{20}N_4O_2S$	228–232	62	−7.1890	−53.5692	168	N- of quinoxaline and H atom of amino acid backbone of MET-1160 S=O of sulphonamido with H atom of amino acid Tyr-1159 NH of sulphonamido with carbonyl oxygen of Lys-1161

Table 1 (*continued*)

S. no.	Compounds	Molecular formula	Melting point (°C)	Percentage yield (%)	Docking score	Glide energy (kcal/mol)	Glide pose	H-bond interaction
3n		$C_{21}H_{17}N_5O_2S_2$	146−148	66	−5.7918	−48.3404	05	N- of quinoxaline and H atom of amino acid backbone of MET-1160 S=O of sulphonamido with H atom of amino acid Tyr-1159 NH of sulphonamido with carbonyl oxygen of Lys-1161
3o		$C_{22}H_{17}N_3O_3S$	162−164	68	−5.2312	−43.2311	193	N- of quinoxaline and H atom of amino acid backbone of MET-1160 S=O of sulphonamido with H atom of amino acid Tyr-1159 NH of sulphonamido with carbonyl oxygen of Lys-1161
3p		$C_{28}H_{21}N_3O_3S$	188−192	62	−8.8983	−58.6781	376	N- of quinoxaline and H atom of amino acid backbone of MET-1160 S=O of sulphonamido with H atom of amino acid Tyr-1159 NH of sulphonamido with carbonyl oxygen of Lys-1161

5. Experimental protocols

All chemicals and solvents were supplied by Merck, S.D. Fine Chemical Limited, Mumbai. All the solvents were distilled and dried before use. The reactions were monitored with the help of thin-layer chromatography using pre-coated aluminum sheets with GF_{254} silica gel, 0.2 mm layer thickness (E. Merck). The solvents used throughout the experiment for running TLC were ethyl acetate and petroleum ether in the ratio of 3:2, chloroform and methanol in the ratio of 9.5:0.5 and 9:1 as developing solvents. UV Cabinet was used for the visualization of TLC spots. Melting points of the synthesized compounds were recorded on the Veego (VMP-MP) melting point apparatus. IR spectrum was acquired on a Shimadzu Infra Red Spectrometer, (model FTIR-8400S). Both ^{1}H NMR (DMSO) and ^{13}C NMR (DMSO) spectra of the synthesized compounds were performed with Bruker Avance-II 400 NMR Spectrometer operating at 400 MHz in SAIF, Punjab University (Chandigarh). Chemical shifts were measured relative to internal standard TMS (δ: 0). Chemical shifts are reported in δ scale (ppm). Mass spectra of the synthesized compounds were recorded at MAT 120 in SAIF, Punjab University.

5.1. Synthesis of 2,3-diphenylquinoxaline-6-sulfonyl chloride (2)

It is prepared as per the procedure mentioned by Ganapaty et al. [27].

5.2. General procedure for the synthesis of N-substituted-2,3-diphenylquinoxaline-6-sulfonamide 3(a−p)

A primary amino containing moiety (0.01 mol) was refluxed with 2,3-diphenylquinoxaline-6-sulfonylchloride **2** (0.01 mol) in 50 mL of 10% aq. NaOH solution for 5 h. The reaction mixture was poured into the crushed ice and stirred until product solidifies; it was then filtered, washed with dilute NaOH solution and recrystallized from ethanol.

5.2.1. N-(2,3-Diphenylquinoxalin-6-ylsulfonyl) acetamide (3a)

IR (KBr) ν_{max} 3345.36 (NH stretch), 3056.44 (CH Arom.), 2934.48 (CH Aliph.), 1660.64 (C=O), 1582.34 (NH bend), 1347.66, 1174.97 (S=O) cm^{-1}; ^{1}H NMR (DMSO-d_6) δ ppm: 10.21 (br s, 1H, NH), 7.32−8.39 (m, 13H, Ar−H), 2.48 (s, 3H, CH$_3$); ^{13}C NMR (DMSO-d_6) δ ppm: 169.56, 156.23, 146.78, 145.24, 143.63, 139.24, 130.62, 129.24, 128.21, 127.24, 126.12, 125.24, 21.26; HRMS (EI) m/z calcd for $C_{22}H_{17}N_3O_3S$: 403.0991; found: 403.0995.
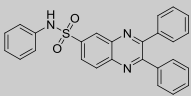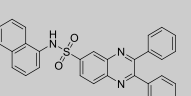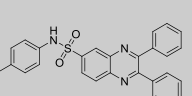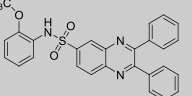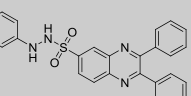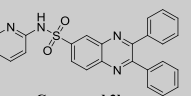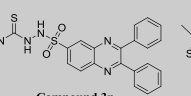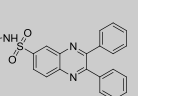
5.2.2. N-(2,3-Diphenylquinoxalin-6-ylsulfonyl) benzamide (3b)

IR (KBr) ν_{max} 3413.91 (NH stretch), 3046.83 (CH stretch), 1672.74 (C=O), 1592.63 (NH bend), 1350.19, 1141.94 (S=O) cm^{-1}; ^{1}H NMR (DMSO-d_6) δ ppm: 10.34 (br s, 1H, NH), 7.21−8.38 (m, 18H, Ar−H); ^{13}C NMR (DMSO-d_6) δ ppm: 169. 78, 158.47, 148.74, 145.46, 144.84, 141.93, 136.53, 133.74, 130.35, 129.75, 128.84, 128.33, 127.83, 127.22, 126.74, 125.23; HRMS (EI) m/z calcd for $C_{27}H_{19}N_3O_3S$: 465.1147; found: 465.1151.

5.2.3. N-(Naphthalen-1-yl)-2,3-diphenylquinoxaline-6-sulfonamide (3c)

IR (KBr) ν_{max} 3343.00 (NH stretch), 3055.85 (CH stretch), 1681.56 (C=O), 1598.56 (NH bend), 1345.14, 1164.91 (S=O) cm^{-1}; ^{1}H NMR (DMSO-d_6) δ ppm: 7.22−8.16 (m, 20H, Ar−H), 5.31 (br s, 1H, NH); ^{13}C NMR (DMSO-d_6) δ ppm: 158.78, 147.34, 145.24, 141.54, 140.20, 139.45, 135.32, 130.64, 129.75, 128.23, 128.11, 127.08, 127.03, 126.65, 126.25, 126.02, 125.74, 124.23, 122.01, 118.64, 109.44; HRMS (EI) m/z calcd for $C_{30}H_{21}N_3O_2S$: 487.1354; found: 487.1358.

Table 2

Percentage growth inhibition (GI %) of in vitro subpanel tumor cell lines at 10^{-5} μM (Single Dose Assay).

Compound → / Cancer Cell Line ↓	Compound 3b NSC:763437	Compound 3c NSC:763438	Compound 3f NSC:763442	Compound 3i NSC: 763441	Compound 3j NSC:763440	Compound 3l NSC:763439	Compound 3n NSC:763435	Compound 3o NSC:763436
Leukemia								
CCRF-CEM	41.34	58.32	61.94	49.84	32.64	70.73	35.83	24.82
HL-60(TB)	49.43	70.98	66.73	60.73	39.92	80.72	40.63	35.26
K-562	45.75	49.56	55.63	45.52	34.92	64.42	34.82	26.83
MOLT-4	44.86	47.78	60.82	56.93	35.52	86.83	28.12	20.54
RPMI-8226	58.54	44.34	86.04	65.72	47.78	89.93	46.37	39.62
SR	71.12	81.12	88.12	81.92	53.78	-3.25	49.98	40.95
Non-Small Cell Lung Cancer								
A549/ATCC	21.12	15.34	41.93	36.45	17.57	54.67	34.72	7.74
EKVX	26.54	71.23	57.83	48.82	30.57	80.82	23.72	8.53
HOP-62	2.87	2.24	12.83	2.12	2.52	22.76	38.73	2.84
NCI-H226	61.97	43.97	-2.45	69.93	59.84	-1.38	52.93	53.64
NCI-H23	19.56	21.34	26.64	23.03	16.56	46.52	11.62	11.67
NCI-H322M	20.87	22.23	32.82	23.23	10.77	59.42	2.92	17.83
NCI-H460	31.97	23.56	47.12	45.54	26.63	63.42	15.63	8.63
NCI-H522	23.54	47.82	50.83	28.82	18.67	65.63	13.74	3.73
Colon Cancer								
COLO 205	19.54	27.87	26.64	28.94	12.67	54.23	4.83	4.64
HCC-2998	15.32	4.56	37.92	19.92	1.83	60.63	8.92	6.23
HCT-116	36.67	49.87	59.62	55.72	36.56	72.12	17.83	14.53
HCT-15	44.94	34.34	44.72	44.72	32.53	62.43	29.92	26.21
HT 29	48.43	82.45	70.43	63.92	39.61	81.72	30.82	21.46
KM 12	20.98	29.92	38.74	8.62	6.93	61.52	15.92	16.75
SW-620	17.43	26.78	30.32	21.54	13.56	47.92	3.72	3.84
CNS Cancer								
SF-268	6.89	2.78	14.12	23.82	1.63	27.63	2.92	1.86
SF-295	20.98	3.88	40.73	15.92	14.52	76.83	8.92	5.83
SF-539	3.89	5.57	25.93	24.72	7.76	61.92	21.72	3.29
SNB-19	21.98	9.78	31.93	41.92	16.52	43.63	14.82	2.12
SNB-75	34.67	39.88	45.12	31.93	29.64	61.82	25.63	26.85
U251	21.56	7.23	39.45	ND	15.62	56.53	26.82	10.32
Melanoma								
LOX IMVI	20.54	32.87	38.42	23.34	15.34	63.32	11.23	12.23
MALME-3M	7.67	9.98	6.64	1.87	2.94	32.85	2.94	2.85
M14	2.45	2.23	30.96	25.98	4.84	62.84	4.23	2.85
MDA-MB-435	12.89	20.45	35.63	22.53	7.72	54.24	11.13	4.73
SK-MEL-2	15.84	14.87	23.93	24.97	2.94	39.29	7.94	8.53
SK-MEL-28	7.63	5.98	14.64	12.67	4.26	30.29	6.93	1.73
SK-MEL-5	48.93	48.56	73.95	61.42	42.28	-6.25	39.13	28.93
UACC-257	15.24	21.66	17.85	18.87	1.94	42.45	8.83	2.23
UACC-62	19.65	28.86	30.56	23.42	30.23	41.13	24.34	20.72
Ovarian Cancer								
IGROV1	16.54	1.78	20.83	11.78	1.84	31.82	8.83	14.84
OVCAR-3	19.25	30.88	28.84	13.46	2.86	48.92	1.84	1.94
OVCAR-4	16.53	31.23	30.28	29.98	17.25	40.12	16.54	13.43
OVCAR-5	8.43	2.98	18.28	12.73	5.94	24.34	4.85	2.84
OVCAR-8	8.02	20.56	34.84	24.12	4.27	52.75	5.83	3.93
NCI/ADR-RES	27.53	22.62	55.21	40.98	13.26	73.20	11.88	8.63
SK-OV-3	12.83	5.86	18.48	18.63	2.37	44.93	5.98	4.85

Cell line								
Renal Cancer								
786-0	2.83	2.34	99.23	25.74	41.54	66.93	4.34	16.54
A-498	22.73	26.75	70.23	33.38	42.83	44.29	31.85	42.22
ACHN	16.62	01.83	34.34	7.63	13.12	23.93	21.89	11.84
CAKI-1	5.83	2.94	54.12	3.23	23.87	33.93	3.34	7.22
RXF-393	14.53	29.24	-40.38	30.27	70.66	98.83	48.64	39.12
SN12C	2.83	6.98	38.49	10.45	32.65	26.93	8.87	17.43
TK-10	6.93	2.74	30.23	1.25	1.26	2.84	6.34	2.54
UO-31	10.63	13.73	45.23	2.23	22.84	29.25	17.86	15.23
Prostate Cancer								
PC-3	33.93	34.64	72.19	34.43	52.82	60.03	41.76	41.85
DU-145	2.63	2.73	37.43	3.74	18.85	24.38	10.87	6.85
Breast Cancer								
MCF7	11.84	18.93	65.94	18.75	31.84	47.74	22.97	22.94
MDA-MB-231/ATCC	14.78	17.63	80.12	30.54	48.28	54.28	38.66	28.54
HS 578T	20.84	6.63	76.34	27.23	33.23	37.54	23.97	16.97
BT-549	2.74	1.83	80.25	35.65	55.13	77.75	32.56	7.67
T-47D	40.64	42.62	81.12	50.93	63.94	72.13	49.43	57.45
MDA-MB-468	23.66	30.83	-4.67	35.13	56.83	76.75	54.87	40.23

Note: Growth percentage inhibition is measured at a single dose of 10 µM concentration; % inhibition is calculated by simple abstraction of the % growth promotion from 100; a pink colour reading shows the five dose selected compounds.

5.2.4. N-(Naphthalen-2-yl)-2,3-diphenylquinoxaline-6-sulfonamide (**3d**)

IR (KBr) ν_{max} 3422.14 (NH stretch), 3056.08 (CH stretch), 1673.78 (C=O), 1601.68 (NH bend), 1362.72, 1162.25 (S=O) cm^{-1}; ^{1}H NMR (DMSO-d_6) δ ppm: 7.32–8.14 (m, 20H, Ar–H), 5.38 (br s, 1H, NH); ^{13}C NMR (DMSO-d_6) δ ppm: 158.46, 148.34, 145.24, 143.34, 142.25, 140.66, 135.78, 130.63, 129.18, 129.08, 128.35, 127.74, 126.78, 126.58, 126.46, 126.02, 125.48, 124.38, 122.44, 119.14, 108.14; HRMS (EI) m/z calcd for $C_{30}H_{21}N_3O_2S$: 487.1354; found: 487.1359.

5.2.5. N-(4-Hydroxyphenyl)-2,3-diphenylquinoxaline-6-sulfonamide (**3e**)

IR (KBr) ν_{max} 3564.48 (OH stretch), 3423.24 (NH stretch), 3050.81 (CH stretch), 1668.24 (C=O), 1578.24 (NH bend), 1332.23, 1168.57 (S=O) cm^{-1}; ^{1}H NMR (DMSO-d_6) δ ppm: 7.12–8.46 (m, 17H, Ar–H), 5.68 (s, 1H, OH), 4.56 (br s, 1H, OH); ^{13}C NMR (DMSO-d_6) δ ppm: 158.57, 149.34, 148.43, 145.63, 142.84, 138.64, 134.95, 130.63, 129.63, 128.54, 127.21, 126.64, 126.22, 125.42, 119.22; HRMS (EI) m/z calcd for $C_{26}H_{19}N_3O_3S$: 453.1147; found: 453.1151.

5.2.6. N-(4-Chlorophenyl)-2,3-diphenylquinoxaline-6-sulfonamide (**3f**)

IR (KBr) ν_{max} 3429.83 (NH stretch), 3028.34 (CH stretch), 1672.58 (C=O), 1588.65 (NH bend), 1350.67, 1180.24 (S=O), 763.42 (C–Cl) cm^{-1}; ^{1}H NMR (DMSO-d_6) δ ppm: 7.04–8.10 (m, 17H, Ar–H), 5.26 (br s, 1H, NH); ^{13}C NMR (DMSO-d_6) δ ppm: 158.64, 148.42, 144.73, 142.63, 140.56, 138.34, 134.78, 133.23, 132.67, 130.24, 129.78, 128.56, 127.34, 126.22, 122.56; HRMS (EI) m/z calcd for $C_{26}H_{18}ClN_3O_2S$: 471.0808; found: 471.0804.

5.2.7. N-(4-Nitrophenyl)-2,3-diphenylquinoxaline-6-sulfonamide (**3g**)

IR (KBr) ν_{max} 3472.91 (NH stretch), 3048.89 (CH stretch), 1675.87 (C=O), 1568.28 (NH bend), 1549.23, 1348.83 (NO$_2$), 1337.76, 1180.26 (S=O) cm^{-1}; ^{1}H NMR (DMSO-d_6) δ ppm: 7.34–8.25 (m, 17H, Ar–H), 5.56 (br s, 1H, NH); ^{13}C NMR (DMSO-d_6) δ ppm: 159.68, 149.24, 146.45, 144.24, 142.78, 140.34, 138.24, 130.78, 129.45, 128.28, 127.84, 126.45, 125.68, 124.46, 119.34; HRMS (EI) m/z calcd for $C_{26}H_{18}N_4O_4S$: 482.1049; found: 482.1053.

5.2.8. N-(3-Nitrophenyl)-2,3-diphenylquinoxaline-6-sulfonamide (**3h**)

IR (KBr) ν_{max} 3414.12 (NH stretch), 3050.82 (CH stretch), 1678.34 (C=O), 1592.78 (NH bend), 1546.23, 1354.68 (NO$_2$), 1338.78, 1174.86 (S=O) cm^{-1}; ^{1}H NMR (DMSO-d_6) δ ppm: 7.37–8.13 (m, 17H, Ar–H), 5.48 (br s, 1H, NH); ^{13}C NMR (DMSO-d_6) δ ppm: 158.56, 150.23, 148.68, 147.38, 145.24, 141.73, 139.28, 134.48, 132.22, 130.64, 129.62, 128.84, 127.53, 126.22, 125.78, 116.34, 115.68; HRMS (EI) m/z calcd for $C_{26}H_{18}N_4O_4S$: 482.1049; found: 482.1045.

5.2.9. N-(2-Methoxyphenyl)-2,3-diphenylquinoxaline-6-sulfonamide (**3i**)

IR (KBr) ν_{max} 3404.34 (NH stretch), 3050.22 (CH stretch), 1684.82 (C=O), 1599.53 (NH bend), 1342.68, 1179.78 (S=O) cm^{-1}; ^{1}H NMR (DMSO-d_6) δ ppm: 7.35–8.19 (m, 17H, Ar–H), 5.34 (br s, 1H, NH), 3.81 (s, 3H, OCH$_3$); ^{13}C NMR (DMSO-d_6) δ ppm: 159.88, 151.34, 148.87, 145.46, 144.78, 140.34, 135.24, 132.88, 130.66, 129.47, 128.84, 127.62, 126.56, 126.22, 124.66, 122.34, 118.24, 55.88; HRMS (EI) m/z calcd for $C_{27}H_{21}N_3O_3S$: 467.1304; found: 467.1309.

5.2.10. N′-2,3-Triphenylquinoxaline-6-sulfonohydrazide (**3j**)

IR (KBr) ν_{max} 3411.83 (NH stretch), 3049.82 (CH stretch), 1662.43 (C=O), 1596.82 (NH bend), 1338.60, 1147.65 (S=O) cm^{-1}; ^{1}H NMR (DMSO-d_6) δ ppm: 7.33–8.21 (m, 18H, Ar–H), 6.45 (s, 1H, NH), 5.12 (s, 1H, SONH); ^{13}C NMR (DMSO-d_6) δ ppm: 158.68, 154.38, 149.44,

National Cancer Institute Developmental Therapeutics Program
In-Vitro Testing Results

NSC : D - 763442 / 1	Experiment ID : 1202NS13	Test Type : 08	Units : Molar
Report Date : August 08, 2012	Test Date : February 21, 2012	QNS :	MC :
COMI : 114502	Stain Reagent : SRB Dual-Pass Related	SSPL : 0YJH	

| | | | | Log10 Concentration | | | | | | | | | | |
| | Time | | Mean Optical Densities | | | | | Percent Growth | | | | | | |
Panel/Cell Line	Zero	Ctrl	-8.0	-7.0	-6.0	-5.0	-4.0	-8.0	-7.0	-6.0	-5.0	-4.0	GI50	TGI	LC50
Leukemia															
CCRF-CEM	0.592	2.069	1.887	1.940	1.766	0.354	1.539	88	91	79	-40	64	.	.	> 1.00E-4
HL-60(TB)	1.003	2.945	2.877	2.918	2.723	0.681	1.869	97	99	89	-32	45	2.09E-6	.	> 1.00E-4
K-562	0.410	2.217	2.188	2.185	2.125	0.603	1.453	98	98	95	11	58	.	> 1.00E-4	> 1.00E-4
MOLT-4	0.649	2.268	2.217	2.177	2.046	0.399	1.748	97	94	86	-39	68	.	.	> 1.00E-4
RPMI-8226	0.985	2.313	2.356	2.331	1.882	0.541	1.512	103	101	68	-45	40	1.43E-6	.	> 1.00E-4
SR	0.663	1.796	1.711	1.656	1.580	0.347	1.232	92	88	81	-48	50	.	.	> 1.00E-4
Non-Small Cell Lung Cancer															
A549/ATCC	0.366	1.782	1.698	1.746	1.600	0.434	1.403	94	97	87	5	73	.	> 1.00E-4	> 1.00E-4
EKVX	0.800	1.826	1.797	1.825	1.738	0.745	1.467	97	100	91	-7	65	.	.	> 1.00E-4
HOP-62	0.286	0.847	0.825	0.845	0.873	0.360	0.532	96	100	105	13	44	3.95E-6	> 1.00E-4	> 1.00E-4
HOP-92	0.534	0.945	0.930	0.913	0.855	0.462	0.665	96	92	78	-13	32	2.03E-6	.	> 1.00E-4
NCI-H226	0.736	1.516	1.445	1.509	1.527	0.524	1.302	91	99	101	-29	73	.	.	> 1.00E-4
NCI-H23	0.533	1.641	1.605	1.553	1.472	0.576	1.333	97	92	85	4	72	.	> 1.00E-4	> 1.00E-4
NCI-H322M	0.775	1.490	1.438	1.475	1.473	1.043	1.408	93	98	98	37	88	.	> 1.00E-4	> 1.00E-4
NCI-H460	0.274	2.358	2.374	2.452	2.239	0.225	1.695	101	105	94	-18	68	.	.	> 1.00E-4
NCI-H522	0.702	1.888	1.804	1.767	1.744	0.465	1.501	93	90	88	-34	67	.	.	> 1.00E-4
Colon Cancer															
COLO 205	0.502	2.054	2.062	2.073	2.099	0.446	1.631	101	101	103	-11	73	.	.	> 1.00E-4
HCC-2998	0.739	2.616	2.605	2.590	2.658	0.778	2.337	99	99	102	2	85	.	> 1.00E-4	> 1.00E-4
HCT-116	0.221	1.602	1.550	1.459	1.324	0.236	0.945	96	90	80	1	52	.	> 1.00E-4	> 1.00E-4
HCT-15	0.468	2.268	2.274	2.241	2.032	0.513	1.695	100	98	87	3	68	.	> 1.00E-4	> 1.00E-4
HT29	0.187	0.978	0.981	0.975	0.862	0.084	0.610	100	100	85	-55	53	.	.	.
KM12	0.455	2.036	2.085	1.944	2.068	0.529	1.572	103	94	102	5	71	.	> 1.00E-4	> 1.00E-4
SW-620	0.241	1.488	1.405	1.381	1.337	0.412	1.113	93	91	88	14	70	.	> 1.00E-4	> 1.00E-4
CNS Cancer															
SF-268	0.565	1.759	1.688	1.734	1.676	0.884	1.468	94	98	93	27	76	.	> 1.00E-4	> 1.00E-4
SF-295	0.996	2.111	2.017	2.004	1.905	0.472	1.857	92	90	82	-53	77	.	.	.
SF-539	0.661	1.927	1.918	1.878	1.940	0.721	1.590	99	96	101	5	73	.	> 1.00E-4	> 1.00E-4
SNB-19	0.569	1.747	1.749	1.698	1.616	0.765	1.549	100	96	89	17	83	.	> 1.00E-4	> 1.00E-4
SNB-75	0.784	1.408	1.255	1.206	1.213	0.856	1.069	75	68	69	12	46	2.12E-6	> 1.00E-4	> 1.00E-4
U251	0.360	1.566	1.525	1.500	1.415	0.344	1.271	97	94	87	-5	75	.	.	> 1.00E-4
Melanoma															
LOX IMVI	0.195	1.784	1.764	1.761	1.602	0.235	1.252	99	99	89	3	66	.	> 1.00E-4	> 1.00E-4
MALME-3M	0.531	0.927	0.950	0.924	0.938	0.304	0.958	106	99	103	-43	108	.	.	> 1.00E-4
M14	0.367	1.309	1.263	1.168	1.253	0.267	1.092	95	85	94	-27	77	.	.	> 1.00E-4
MDA-MB-435	0.382	1.641	1.599	1.544	1.543	0.288	1.336	97	92	92	-25	76	.	.	> 1.00E-4
SK-MEL-2	0.548	0.942	0.914	0.939	0.936	0.241	0.822	93	99	99	-56	69	.	.	.
SK-MEL-28	0.592	1.647	1.617	1.610	1.555	0.811	1.456	97	96	91	21	82	.	> 1.00E-4	> 1.00E-4
SK-MEL-5	0.657	2.027	1.963	1.961	1.790	0.009	1.371	95	95	83	-99	52	.	.	.
UACC-257	0.603	1.340	1.295	1.334	1.221	0.461	1.096	94	99	84	-24	67	.	.	> 1.00E-4
UACC-62	0.606	2.289	2.204	2.073	1.883	0.473	1.657	95	87	76	-22	62	.	.	> 1.00E-4
Ovarian Cancer															
IGROV1	0.653	1.952	1.972	1.959	1.861	0.968	1.597	102	101	93	24	73	.	> 1.00E-4	> 1.00E-4
OVCAR-3	0.508	1.575	1.579	1.545	1.515	0.302	1.207	100	97	94	-41	65	.	.	> 1.00E-4
OVCAR-4	0.434	0.837	0.775	0.795	0.739	0.481	0.642	85	90	76	12	52	.	> 1.00E-4	> 1.00E-4
OVCAR-5	0.594	1.357	1.321	1.299	1.277	0.636	1.285	95	92	90	6	90	.	> 1.00E-4	> 1.00E-4
OVCAR-8	0.356	1.449	1.405	1.457	1.360	0.419	1.142	96	101	92	6	72	.	> 1.00E-4	> 1.00E-4
NCI/ADR-RES	0.408	1.537	1.530	1.560	1.409	0.412	1.185	99	102	89	.	69	.	> 1.00E-4	> 1.00E-4
SK-OV-3	0.497	1.153	1.121	1.148	1.184	0.586	0.925	95	99	105	14	65	.	> 1.00E-4	> 1.00E-4
Renal Cancer															
786-0	0.576	2.028	1.980	1.851	1.920	0.315	1.669	97	88	93	-45	75	.	.	> 1.00E-4
A498	1.116	1.746	1.590	1.596	1.527	1.058	1.497	75	76	65	-5	61	.	.	> 1.00E-4
ACHN	0.541	2.018	2.042	1.942	1.954	0.626	1.658	102	95	96	6	76	.	> 1.00E-4	> 1.00E-4
CAKI-1	0.748	1.816	1.679	1.689	1.700	0.486	1.439	87	88	89	-35	65	.	.	> 1.00E-4
RXF 393	0.646	1.087	1.072	1.101	1.077	0.383	0.871	97	103	98	-41	51	.	.	> 1.00E-4
SN12C	0.508	2.155	2.066	2.095	2.046	0.861	1.796	95	96	93	21	78	.	> 1.00E-4	> 1.00E-4
TK-10	0.594	1.183	1.126	1.177	1.232	0.649	1.100	90	99	108	9	86	.	> 1.00E-4	> 1.00E-4
UO-31	0.621	1.610	1.485	1.501	1.508	0.679	1.362	87	89	90	6	75	.	> 1.00E-4	> 1.00E-4
Prostate Cancer															
PC-3	0.434	1.492	1.389	1.408	1.096	0.380	0.874	90	92	63	-12	42	1.47E-6	.	> 1.00E-4
DU-145	0.357	1.413	1.460	1.397	1.340	0.634	1.046	105	99	93	26	65	.	> 1.00E-4	> 1.00E-4
Breast Cancer															
MCF7	0.448	2.179	2.098	2.101	2.066	0.376	1.757	95	95	93	-16	76	.	.	> 1.00E-4
MDA-MB-231/ATCC	0.411	1.114	1.107	1.124	0.993	0.090	0.789	99	101	83	-78	54	.	.	.
HS 578T	0.926	1.701	1.580	1.685	1.512	0.953	1.385	84	98	76	3	59	.	> 1.00E-4	> 1.00E-4
BT-549	0.785	1.681	1.659	1.513	1.486	0.627	1.331	98	81	78	-20	61	.	.	> 1.00E-4
T-47D	0.766	1.450	1.413	1.384	1.235	0.612	1.021	95	90	69	-20	37	1.62E-6	.	> 1.00E-4

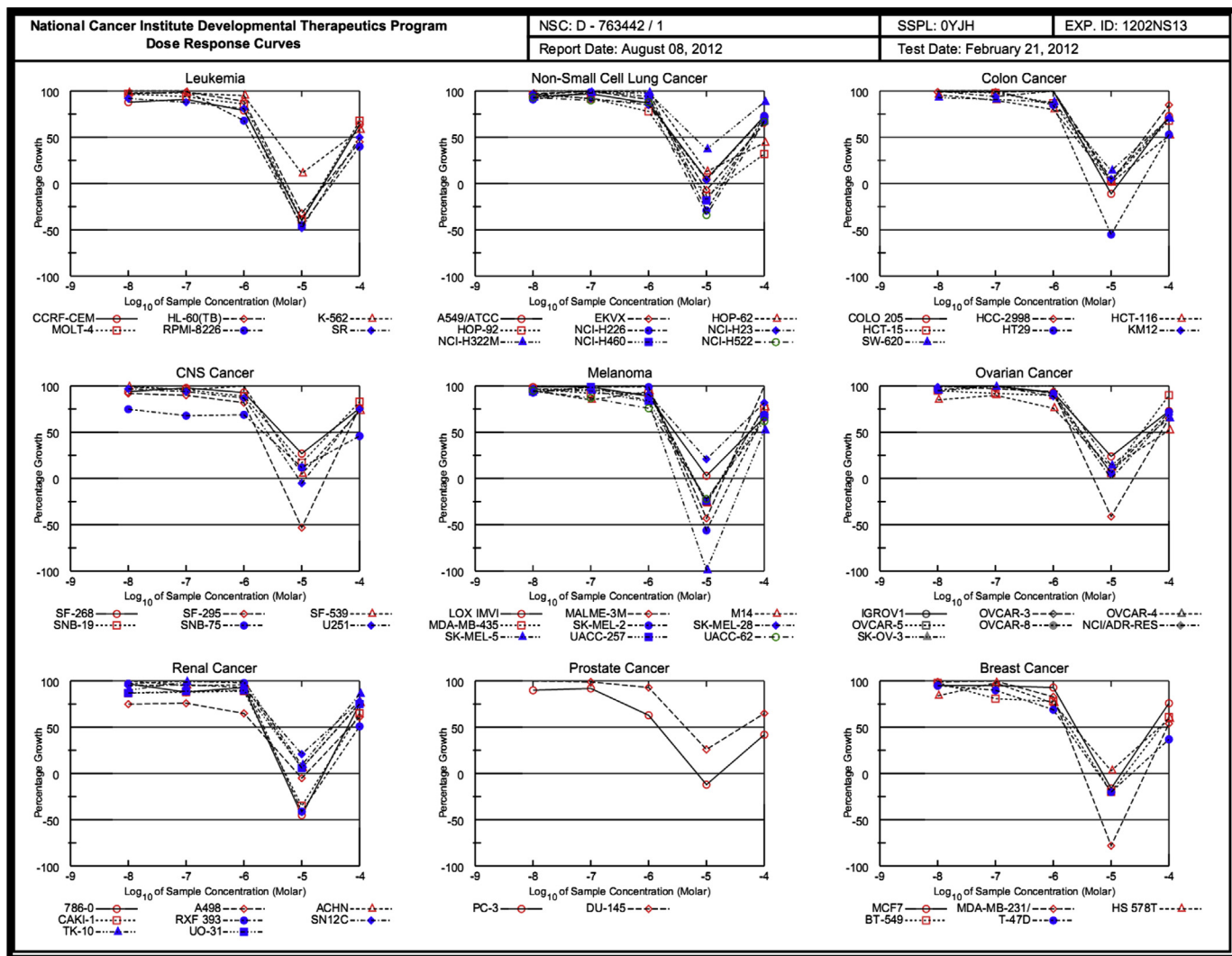**Fig. 5.** Five dose assay of compound **3f** (NSC: 763442).

Fig. 6. Five dose assay graph of compound **3f** (NSC: 763442) against nine panel cancer cell line at NCI.

145.77, 142.73, 140.98, 132.38, 131.34, 130.48, 129.24, 128.52, 126.63, 125.28, 122.18, 113.24; HRMS (EI) m/z calcd for $C_{26}H_{20}N_4O_2S$: 452.1307; found: 452.1312.

5.2.11. 2-(2,3-Diphenylquinoxaline-6-sulfonamido)benzoic acid (3k)

IR (KBr) ν_{max} 3385.33 (OH acid), 3327.28 (NH stretch), 3055.28 (CH stretch), 1645.83 (C=O), 1578.82 (NH bend), 1346.62, 1146.63 (S=O) cm^{-1}; ^{1}H NMR (DMSO-d_6) δ ppm: 10.21 (s, 1H, OH), 7.25–8.21 (m, 17H, Ar–H), 5.34 (s, 1H, NH$_2$); ^{13}C NMR (DMSO-d_6) δ ppm: 170.68, 156.88, 149.34, 146.48, 145.18, 143.57, 140.32, 138.47, 135.14, 132.86, 131.28, 129.78, 128.57, 127.36, 126.24, 119.24, 116.21, 112.28; HRMS (EI) m/z calcd for $C_{27}H_{19}N_3O_4S$: 481.1096; found: 481.1091.

5.2.12. 2,3-Diphenyl-N-(pyridin-2-yl)quinoxaline-6-sulfonamide (3l)

IR (KBr) ν_{max} 3409.28 (NH stretch), 3056.26 (CH stretch), 1658.84 (C=O), 1588.82 (NH bend), 1356.34, 1148.65 (S=O) cm^{-1}; ^{1}H NMR (DMSO-d_6) δ ppm: 7.30–8.25 (m, 17H, Ar–H), 5.49 (br s, 1H, NH); ^{13}C NMR (DMSO-d_6) δ ppm: 158.78, 155.24, 150.78, 148.36, 145.44, 143.44, 140.23, 139.93, 132.24, 131.68, 129.48, 128.34, 127.28, 126.38, 118.28, 109.19; HRMS (EI) m/z calcd for $C_{25}H_{18}N_4O_2S$: 438.1150; found: 438.1155.

5.2.13. N-(4-Methylpyridin-2-yl)-2,3-diphenylquinoxaline-6-sulfonamide (3m)

IR (KBr) ν_{max} 3408.24 (NH stretch), 3018.78 (CH Arom.), 2918.34 (CH Alip.), 1663.68 (C=O), 1581.64 (NH bend), 1352.78, 1152.63 (S=O) cm^{-1}; ^{1}H NMR (DMSO-d_6) δ ppm: 7.35–8.25 (m, 16H, Ar–H), 5.31 (br s, 1H, NH), 2.11 (s, 3H, CH$_3$); ^{13}C NMR (DMSO-d_6) δ ppm: 158.48, 154.48, 152.68, 149.38, 146.58, 145.48, 144.58, 140.38, 135.58, 132.47, 130.23, 129.57, 128.56, 127.23, 122.12, 118.57, 22.45; HRMS (EI) m/z calcd for $C_{26}H_{20}N_4O_2S$: 452.1307; found: 452.1303.

5.2.14. 2-(2,3-Diphenylquinoxalin-6-ylsulfonyl) hydrazinecarbothioamide (3n)

IR (KBr) ν_{max} 3398.9 (NH stretch), 3034.24 (CH stretch), 1676.24 (C=O), 1572.88 (NH bend), 1358.24, 1162.34 (S=O) cm^{-1}; ^{1}H NMR (DMSO-d_6) δ ppm: 7.15–8.16 (m, 13H, Ar–H), 10.12 (s, 2H, NH$_2$), 5.12 (s, 1H, NH), 4.42 (s, 1H, NH); ^{13}C NMR (DMSO-d_6) δ ppm: 179.56, 158.48, 148.85, 144.24, 142.68, 140.49, 134.23, 132.56, 130.29, 129.58, 128.45, 126.56; HRMS (EI) m/z calcd for $C_{21}H_{17}N_5O_2S_2$: 435.0824; found: 435.0829.

5.2.15. N-(2,3-Diphenylquinoxalin-6-ylsulfonyl)ethanethioamide (3o)

IR (KBr) ν_{max} 3424.26 (NH stretch), 3035.56 (CH Arom.), 2934.56 (CH Alip.), 1668.24 (C=O), 1596.22 (NH bend), 1356.34,

National Cancer Institute Developmental Therapeutics Program
In-Vitro Testing Results

NSC : D - 763439 / 1	Experiment ID : 1202NS13	Test Type : 08	Units : Molar
Report Date : August 08, 2012	Test Date : February 21, 2012	QNS :	MC :
COMI : 114496	Stain Reagent : SRB Dual-Pass Related	SSPL : 0YJH	

			Log10 Concentration											
	Time		Mean Optical Densities					Percent Growth						
Panel/Cell Line	Zero	Ctrl	-8.0	-7.0	-6.0	-5.0	-4.0	-8.0	-7.0	-6.0	-5.0	-4.0	GI50	TGI	LC50
Leukemia															
HL-60(TB)	1.003	2.880	2.841	2.819	2.398	0.705	1.539	98	97	74	-30	29	1.71E-6	.	> 1.00E-4
K-562	0.410	2.170	2.260	2.148	1.848	0.562	1.253	105	99	82	9	48	2.72E-6	> 1.00E-4	> 1.00E-4
MOLT-4	0.649	2.153	2.093	2.081	1.852	0.463	1.374	96	95	80	-29	48	1.89E-6	.	> 1.00E-4
RPMI-8226	0.985	2.012	2.096	2.057	1.548	0.509	1.258	108	104	55	-48	27	1.11E-6	.	> 1.00E-4
SR	0.663	1.726	1.652	1.609	1.364	0.383	0.857	93	89	66	-42	18	1.40E-6	.	> 1.00E-4
Non-Small Cell Lung Cancer															
A549/ATCC	0.366	1.639	1.572	1.613	1.591	0.485	1.012	95	98	96	9	51	.	> 1.00E-4	> 1.00E-4
EKVX	0.800	1.806	1.804	1.793	1.699	0.782	1.303	100	99	89	-2	50	2.69E-6	.	> 1.00E-4
HOP-62	0.286	0.757	0.757	0.779	0.849	0.365	0.475	96	101	115	16	39	4.54E-6	> 1.00E-4	> 1.00E-4
HOP-92	0.534	0.839	0.820	0.814	0.770	0.439	0.537	94	92	77	-18	1	1.94E-6	.	> 1.00E-4
NCI-H226	0.736	1.406	1.403	1.369	1.377	0.475	1.203	100	95	96	-35	70	.	.	> 1.00E-4
NCI-H23	0.533	1.568	1.511	1.503	1.352	0.579	0.972	95	94	79	4	42	2.45E-6	> 1.00E-4	> 1.00E-4
NCI-H322M	0.775	1.412	1.387	1.422	1.462	0.996	1.188	96	102	108	35	65	.	> 1.00E-4	> 1.00E-4
NCI-H460	0.274	2.286	2.365	2.405	2.159	0.298	1.580	104	106	94	1	65	.	> 1.00E-4	> 1.00E-4
NCI-H522	0.702	1.873	1.748	1.731	1.563	0.409	1.060	89	88	74	-42	31	1.60E-6	.	> 1.00E-4
Colon Cancer															
COLO 205	0.502	1.899	1.878	1.870	1.814	0.135	1.304	98	98	94	-73	57	.	.	> 1.00E-4
HCC-2998	0.739	2.522	2.504	2.522	2.513	0.639	1.876	99	100	100	-14	64	.	.	> 1.00E-4
HCT-116	0.221	1.438	1.396	1.282	1.129	0.239	0.697	97	87	75	1	39	2.17E-6	> 1.00E-4	> 1.00E-4
HCT-15	0.468	2.206	2.209	2.164	1.816	0.527	1.558	100	98	78	3	63	.	> 1.00E-4	> 1.00E-4
HT29	0.187	0.861	0.877	0.840	0.719	0.119	0.351	102	97	79	-37	24	1.78E-6	.	> 1.00E-4
KM12	0.455	1.898	1.771	1.886	1.887	0.546	1.218	91	99	99	6	53	.	> 1.00E-4	> 1.00E-4
SW-620	0.241	1.400	1.408	1.428	1.255	0.399	0.929	101	102	87	14	59	.	> 1.00E-4	> 1.00E-4
CNS Cancer															
SF-268	0.565	1.646	1.569	1.548	1.637	0.857	1.256	93	91	99	27	64	.	> 1.00E-4	> 1.00E-4
SF-295	0.996	2.058	1.911	1.959	1.947	0.442	1.416	86	91	90	-56	40	1.87E-6	.	> 1.00E-4
SF-539	0.661	1.821	1.769	1.748	1.776	0.742	1.282	96	94	96	7	54	.	> 1.00E-4	> 1.00E-4
SNB-19	0.569	1.687	1.687	1.608	1.541	0.754	1.266	100	93	87	17	62	.	> 1.00E-4	> 1.00E-4
SNB-75	0.784	1.260	1.187	1.215	1.142	0.799	0.879	85	90	75	3	20	2.23E-6	> 1.00E-4	> 1.00E-4
U251	0.360	1.323	1.312	1.290	1.169	0.381	0.816	99	97	84	2	47	2.61E-6	> 1.00E-4	> 1.00E-4
Melanoma															
LOX IMVI	0.195	1.445	1.404	1.411	1.299	0.014	0.910	97	97	88	-93	57	.	.	.
MALME-3M	0.531	0.848	0.838	0.871	0.894	0.318	0.840	97	107	115	-40	97	.	.	> 1.00E-4
M14	0.367	1.248	1.211	1.153	1.230	0.214	0.979	96	89	98	-42	69	.	.	> 1.00E-4
MDA-MB-435	0.382	1.455	1.442	1.477	1.354	0.286	1.199	99	102	91	-25	76	.	.	> 1.00E-4
SK-MEL-28	0.592	1.459	1.469	1.435	1.423	0.753	1.300	101	97	96	19	82	.	> 1.00E-4	> 1.00E-4
SK-MEL-5	0.657	2.012	1.951	1.901	1.713	0.047	1.215	95	92	78	-93	41	1.46E-6	.	.
UACC-257	0.603	1.169	1.145	1.186	1.060	0.451	0.902	96	103	81	-25	53	.	.	> 1.00E-4
UACC-62	0.606	2.063	1.953	1.948	1.696	0.525	1.541	92	92	75	-13	64	.	.	> 1.00E-4
Ovarian Cancer															
IGROV1	0.653	1.912	1.951	1.967	1.937	1.031	1.441	103	104	102	30	63	.	> 1.00E-4	> 1.00E-4
OVCAR-3	0.508	1.499	1.421	1.419	1.417	0.345	0.953	92	92	92	-32	45	2.17E-6	.	> 1.00E-4
OVCAR-4	0.434	0.741	0.741	0.747	0.685	0.466	0.497	100	102	82	10	21	2.79E-6	> 1.00E-4	> 1.00E-4
OVCAR-5	0.594	1.256	1.210	1.213	1.285	0.649	1.250	93	93	104	8	99	.	> 1.00E-4	> 1.00E-4
OVCAR-8	0.356	1.251	1.255	1.223	1.121	0.358	0.765	100	97	85	.	46	2.60E-6	> 1.00E-4	> 1.00E-4
NCI/ADR-RES	0.408	1.394	1.406	1.409	1.234	0.404	0.979	101	102	84	-1	58	.	.	> 1.00E-4
SK-OV-3	0.497	1.115	1.094	1.102	1.103	0.567	0.726	97	98	98	11	37	3.58E-6	> 1.00E-4	> 1.00E-4
Renal Cancer															
786-0	0.576	1.904	1.906	1.796	1.854	0.405	1.247	100	92	96	-30	50	.	.	> 1.00E-4
A498	1.116	1.736	1.664	1.655	1.528	1.030	1.419	88	87	66	-8	49	1.67E-6	.	> 1.00E-4
ACHN	0.541	1.912	1.902	1.888	1.828	0.618	1.387	99	98	94	6	62	.	> 1.00E-4	> 1.00E-4
CAKI-1	0.748	1.673	1.592	1.610	1.689	0.666	1.422	91	93	102	-11	73	.	.	> 1.00E-4
RXF 393	0.646	1.005	1.023	1.037	0.992	0.362	0.782	105	109	96	-44	38	2.14E-6	.	> 1.00E-4
SN12C	0.508	1.955	1.880	1.848	1.827	0.887	1.430	95	93	91	26	64	.	> 1.00E-4	> 1.00E-4
TK-10	0.594	1.051	1.015	1.048	1.115	0.613	0.840	92	99	114	4	54	.	> 1.00E-4	> 1.00E-4
UO-31	0.621	1.545	1.432	1.434	1.409	0.587	1.163	88	88	85	-5	59	.	.	> 1.00E-4
Prostate Cancer															
PC-3	0.434	1.358	1.330	1.289	0.993	0.382	0.651	97	93	60	-12	23	1.39E-6	.	> 1.00E-4
DU-145	0.357	1.349	1.368	1.336	1.303	0.664	0.938	102	99	95	31	59	.	> 1.00E-4	> 1.00E-4
Breast Cancer															
MCF7	0.448	1.912	1.834	1.855	1.721	0.348	1.040	95	96	87	-22	40	2.18E-6	.	> 1.00E-4
MDA-MB-231/ATCC	0.411	1.015	1.073	1.060	0.947	0.163	0.661	110	107	89	-60	41	1.82E-6	.	.
HS 578T	0.926	1.674	1.618	1.629	1.410	0.822	1.267	93	94	65	-11	46	1.56E-6	.	> 1.00E-4
BT-549	0.785	1.614	1.602	1.455	1.372	0.520	1.194	99	81	71	-34	49	1.58E-6	.	> 1.00E-4
T-47D	0.766	1.271	1.245	1.197	1.038	0.599	0.759	95	85	54	-22	-1	1.12E-6	5.14E-6	> 1.00E-4

Fig. 7. Five dose assay of compound **3l** (NSC: 763439).

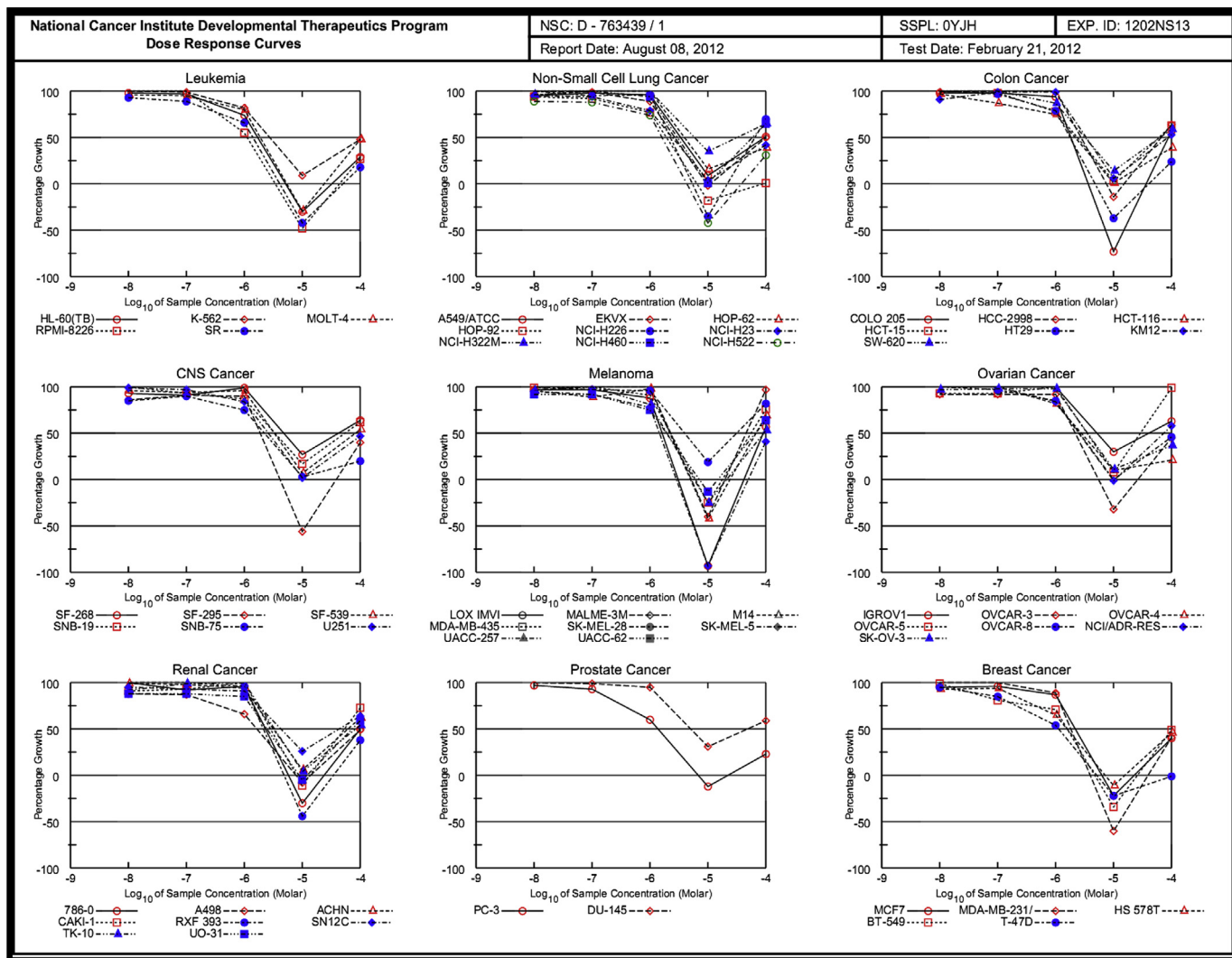**Fig. 8.** Five dose assay graph of compound **3l** (NSC: 763439) against nine panel cancer cell line at NCI.

1162.46 (S=O) cm^{-1}; ^{1}H NMR (DMSO-d_6) δ ppm: 7.32–8.16 (m, 13H, Ar–H), 5.38 (br s, 1H, NH), 2.68 (s, 3H, CH$_3$); ^{13}C NMR (DMSO-d_6) δ ppm: 196.65, 159.34, 149.58, 145.24, 143.56, 140.68, 132.26, 130.88, 129.44, 128.34, 126.61, 125.24, 35.34; HRMS (EI) m/z calcd for C$_{22}$H$_{17}$N$_3$O$_2$S$_2$: 419.0762; found: 419.0766.

### 5.2.16. N-(3-Acetylphenyl)-2,3-diphenylquinoxaline-6-sulfonamide (3p)

IR (KBr) ν_{max} 3444.24 (NH stretch), 3055.24 (CH Arom.), 2901.56 (CH Alip.), 1672.88 (C=O), 1578.24 (NH bend), 1362.22, 1142.78 (S=O) cm^{-1}; ^{1}H NMR (DMSO-d_6) δ ppm: 7.01–8.34 (m, 17H, Ar–H), 5.41 (br s, 1H, NH), 2.58 (s, 3H, CH$_3$); ^{13}C NMR (DMSO-d_6) δ ppm: 194.68, 158.34, 148.24, 144.34, 142.56, 140.68, 138.34, 136.89, 135.34, 132.34, 130.68, 128.46, 127.34, 126.24, 126.02, 122.28, 119.48, 116.48, 24.24; HRMS (EI) m/z calcd for C$_{28}$H$_{21}$N$_3$O$_3$S: 479.1304; found: 479.1309.

5.3. Protocol of in vitro anticancer screening at NCI

The in vitro anticancer screening at NCI is a two-stage process, beginning with the evaluation of all compounds against the 60 cell lines at a single dose of 10 μM. The output from the single dose screen is reported as a mean graph and is available for analysis by the COMPARE program. Compounds which exhibit significant growth inhibition are evaluated against the 60 cell panel at five concentration levels. The human tumor cell lines of the cancer screening panel are grown in RPMI 1640 medium containing 5% fetal bovine serum and 2 mM L-glutamine. For a typical screening experiment, cells are inoculated into 96 well microtiter plates in 100 μL at plating densities ranging from 5000 to 40,000 cells/well depending on the doubling time of individual cell lines. After cell inoculation, the microtiter plates are incubated at 37 °C, 5% CO$_2$, 95% air and 100% relative humidity for 24 h prior to addition of experimental drugs.

After 24 h, two plates of each cell line are fixed *in situ* with TCA, to represent a measurement of the cell population for each cell line at the time of drug addition (Tz). Experimental drugs are solubilized in dimethyl sulfoxide at 400 fold the desired final maximum test concentration and stored frozen prior to use. At the time of drug addition, an aliquot of frozen concentrate is thawed and diluted to twice the desired final maximum test concentration with complete medium containing 50 μg/ml gentamicin. Additional four, 10-fold or ½ log serial dilutions are made to provide a total of five drug concentrations plus control. Aliquots of 100 μl of these different drug dilutions are added to the appropriate microtiter wells already containing 100 μl of medium, resulting in the required final drug concentrations.
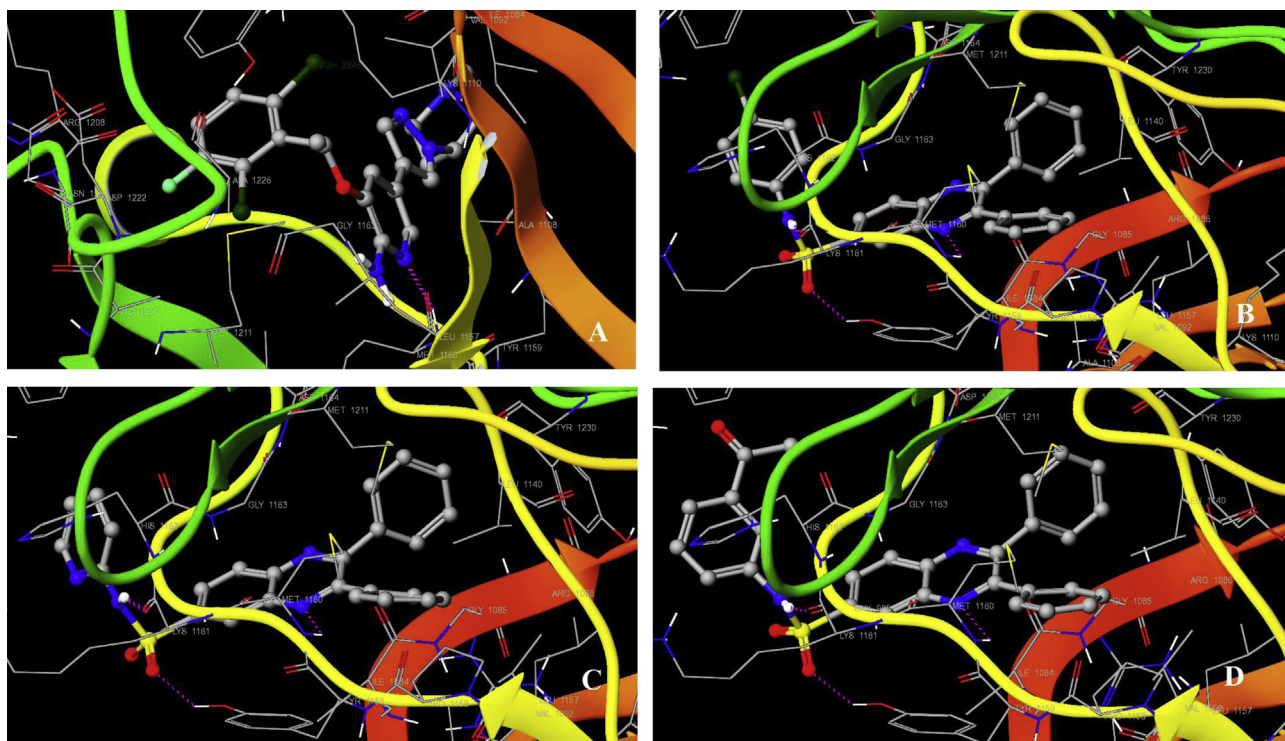
Fig. 9. Binding mode of crizotinib (c-Met Kinsae Inhibitor) H-bond interaction with MET-1160 shown in (A) and compound **3f** (NSC: 763442), (B) **3l** (NSC: 763439), (C) **3p**, (D) showing hydrogen bond interaction with N- of quinoxaline and H atom of amino acid backbone of MET-1160; S=O of sulphonamido with H atom of amino acid Tyr-1159; NH of sulphonamido with carbonyl oxygen of Lys-1161 of c-Met Kinsae receptor (PDB: 2wgj) [H-bonding interaction is shown in pink dotted line]. (For interpretation of the references to colour in this figure legend, the reader is referred to the web version of this article.)

Table 3
Lipinski's rule of five for drug likeliness and in silico ADME properties of **3**(**a**–**p**) by QikProp (Schordinger 9.0).
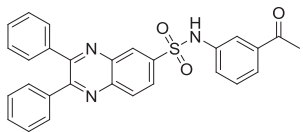
Criteria		Lipinski's rule of five (Drug Likeliness)				In silico ADME by QikProp, Schordinger 9.0				
S. no.	Compounds	Molecular weight	QPlogP O/W[a]	H-Bond donor	H-Bond acceptor	QPlogS[b]	QPlogHERG[c]	QPPCaco[d]	QPMDCK[e]	% Human oral absorption[f]
3a		403.455	3.527	01	7	−5.647	−6.989	427.026	200.927	94.677
3b		465.525	4.772	01	7	−6.788	−8.075	486.878	227.464	100
3c		487.575	5.391	01	6.5	−6.685	−7.708	969.418	479.587	100
3d		487.575	5.504	01	6.5	−6.789	−7.729	981.419	494.532	100

(continued on next page)

Table 3 (continued)

Criteria		Lipinski's rule of five (Drug Likeliness)				In silico ADME by QikProp, Schordinger 9.0				
S. no.	Compounds	Molecular weight	QPlogP O/W[a]	H-Bond donor	H-Bond acceptor	QPlogS[b]	QPlogHERG[c]	QPPCaco[d]	QPMDCK[e]	% Human oral absorption[f]
3e		453.514	3.765	02	7.25	−5.305	−6.97	322.424	147.55	93.886
3f		471.96	4.957	01	6.5	−6.199	−6.961	954.38	1085.791	100
3g		482.513	3.869	01	7.5	−5.716	−7.075	133.383	56.572	87.633
3h		482.513	3.799	01	7.5	−5.848	−7.203	108.407	44.809	85.613
3i		467.541	5.03	01	7.25	−6.358	−7.999	241.673	635.372	100
3j		452.53	4.426	02	7.5	−6.248	−8.018	458.515	318.385	100
3k		481.525	4.756	01	7.5	−6.466	−5.981	40.588	19.782	83.58
3l		438.503	4.03	01	6.5	−4.897	−6.968	460.727	267.902	100
3m		452.53	4.154	01	7.5	−5.628	−6.959	477.758	273.417	100
3n		435.518	2.591	03	09	−5.654	−7.3	156.438	171.476	81.389
3°		403.455	3.531	01	07	−5.657	−7.001	428.521	201.632	94.726

Table 3 (continued)

Criteria		Lipinski's rule of five (Drug Likeliness)				In silico ADME by QikProp, Schordinger 9.0				
S. no.	Compounds	Molecular weight	QPlogP O/W[a]	H-Bond donor	H-Bond acceptor	QPlogS[b]	QPlogHERG[c]	QPPCaco[d]	QPMDCK[e]	% Human oral absorption[f]
3p		479.552	4.068	01	8.5	−5.653	−7.144	377.624	174.263	96.887

[a] Predicted octanol/water partition co-efficient LogP (acceptable range: −2.0–6.5).
[b] Predicted aqueous solubility; S in mol/L (acceptable range: −6.5–0.5).
[c] Predicted IC_{50} value for blockage of HERG K^+ channels (concern below −5.0).
[d] Predicted Caco-2 cell permeability in nm/s (acceptable range: <25 is poor and >500 is great).
[e] Predicted apparent MDCK cell permeability in nm/s.
[f] Percentage of human oral absorption (<25% is poor and >80% is high).

Following the drug addition, the plates are incubated for an additional 48 h at 37 °C, 5% CO_2, 95% air, and 100% relative humidity. For adherent cells, the assay is terminated by the addition of cold TCA. Cells are fixed *in situ* by the gentle addition of 50 μl of cold 50% (w/v) TCA (final concentration, 10% TCA) and incubated for 60 min at 4 °C. The supernatant is discarded, and the plates are washed five times with tap water and air-dried. Sulforhodamine B (SRB) solution (100 μl) at 0.4% (w/v) in 1% acetic acid is added to each well, and plates are incubated for 10 min at room temperature. After staining, unbound dye is removed by washing five times with 1% acetic acid and the plates are air-dried. Bound stain is subsequently solubilized with 10 mM trizma base, and the absorbance is read on an automated plate reader at a wavelength of 515 nm. For suspension cells, the methodology is the same except that the assay is terminated by fixing settled cells at the bottom of the wells by gently adding 50 μl of 80% TCA (final concentration, 16% TCA). Using the seven absorbance measurements [time zero, (Tz), control growth, (C), and test growth in the presence of drug at the five concentration levels (Ti)], the percentage growth is calculated at each of the drug concentrations levels. Percentage growth inhibition is calculated as:

$$[(Ti - Tz)/(C - Tz)] \times 100 \text{ for concentrations for which Ti} \geq Tz$$

$$[(Ti - Tz)/Tz] \times 100 \text{ for concentrations for which Ti} < Tz.$$

Three dose response parameters are calculated for each experimental agent. Growth inhibition of 50% (GI_{50}) is calculated from $[(Ti - Tz)/(C - Tz)] \times 100 = 50$, which is the drug concentration resulting in a 50% reduction in the net protein increase (as measured by SRB staining) in control cells during the drug incubation. The drug concentration resulting in total growth inhibition (TGI) is calculated from Ti = Tz. The LC_{50} (concentration of drug resulting in a 50% reduction in the measured protein at the end of the drug treatment as compared to that at the beginning) indicating a net loss of cells following treatment is calculated from $[(Ti - Tz)/Tz] \times 100 = -50$. Values are calculated for each of these three parameters if the level of activity is reached; however, if the effect is not reached or is exceeded, the value for that parameter is expressed as greater or less than the maximum or minimum concentration tested [33–35].

Acknowledgement

Appendix A. Supplementary data

Supplementary data related to this article can be found at http://dx.doi.org/10.1016/j.ejmech.2013.04.028.

References

[1] H. Yasui, K. Imai, Anti-Cancer Agents Med. Chem. 8 (2008) 470.
[2] M.A. Alaoui-Jamali, Biomed. Pharmacother. 60 (2006) 629.
[3] M.J.A. de Jonge, J. Verweij, Eur. J. Cancer 42 (2006) 1351.
[4] C. Birchmeier, W. Birchmeier, E. Gherardi, G.F. vandeWoude, Nat. Rev. Mol. Cell Biol. 4 (2003) 915.
[5] W.G. Jiang, T.A. Martin, C. Parr, G. Davies, K. Matsumoto, T. Nakamura, Crit. Rev. Oncol. Hematol. 53 (2005) 35.
[6] J.G. Christensen, J. Burrows, R. Salgia, Cancer Lett. 1 (2005) 225.
[7] P.C. Ma, G. Maulik, J. Christensen, R. Salgia, Cancer Metastasis Rev. 22 (2003) 309.
[8] L. Trusolino, A. Bertotti, M.P. Comoglio, Nat. Rev. Mol. Cell Biol. 11 (2010) 834.
[9] J.P. Eder, G.F. VandeWoude, S.A. Boerner, P.M. LoRusso, Clin. Cancer Res. 15 (2009) 2207.
[10] X. Liu, W. Yao, R.C. Newton, P. Scherle, Expert Opin. Investig. Drugs 17 (2008) 997.
[11] O. Abidoye, N. Murukurthy, R. Salgia, Rev. Recent Clin. Trial. 2 (2007) 143.
[12] P.M. Comoglio, S. Giordano, L. Trusolino, Nat. Rev. Drug Discovery 7 (2008) 504.
[13] H.Y. Zou, Q. Li, J.H. Lee, M.E. Arango, S.R. McDonnell, S. Yamazaki, T.B. Koudriakova, G. Alton, J.J. Cui, P.P. Kung, M.D. Nambu, G. Los, S.L. Bender, B. Mroczkowski, J.G. Christensen, Cancer Res. 67 (2007) 4408.
[14] X. Wang, P. Le, C. Liang, J. Chan, D. Kiewlich, T. Miller, D. Harris, L. Sun, A. Rice, S. Vasile, R.A. Blake, A.R. Howlett, N. Patel, G. McMahon, K.E. Lipson, Mol. Cancer Ther. 2 (2003) 1085.
[15] A. Furlan, F. Colombo, A. Kover, N. Issaly, C. Tintori, L. Angeli, V. Leroux, S. Letard, M. Amat, Y. Asses, B. Maigret, P. Dubreuil, M. Botta, R. Dono, J. Bosch, D. Passarella, F. Maina, Eur. J. Med. Chem. 47 (2012) 239–254.
[16] F. Colombo, C. Tintori, A. Furlan, S. Borrelli, M. Christodoulou, R. Dono, F. Maina, M. Botta, M. Amat, J. Bosch, D. Passarella, Bioorg. Med. Chem. Lett. 22 (2012) 4693–4696.
[17] A. Burguete, E. Pontiki, D. Hadjipavlou-Litina, Bioorg. Med. Chem. Lett. 17 (2007) 6439.
[18] A. Levitzki, Acc. Chem. Res. (2003) 462.
[19] J.L. Porter, L. Simon, R. Fabien, F. James, C. Anne, R. Kelly, E. Mark, D. Helen, F. Jean, G.J. Richard, M.M. Jose, M. Alison, B. Christoph, Bioorg. Med. Chem. Lett. 19 (2009) 397.
[20] M.N. Noolvi, H.M. Patel, Eur. J. Med. Chem. 46 (2011) 2327.
[21] M.N. Noolvi, H.M. Patel, Eur. J. Med. Chem. 46 (2011) 4411.
[22] M.N. Noolvi, H.M. Patel, V. Bhardwaj, Med. Chem. 7 (2011) 2002.
[23] M.N. Noolvi, H.M. Patel, Lett. Drug Des. Discovery 7 (2010) 556.
[24] M.N. Noolvi, H.M. Patel, S. Kamboj, A. Kaur, V. Mann, Eur. J. Med. Chem. 56 (2012) 56–69.
[25] M.N. Noolvi, H.M. Patel, M. Kaur, Eur. J. Med. Chem. 54 (2012) 447–462.

[26] H.Y. Zou, Q. Li, J. Lee, M. Arango, S.R. McDonnel, C. Dussell, M. Stempniak, S. Yamazaki, T. Koudriakova, G. Alton, J. Cui, M. Tran-Dube, P.P. Kung, M. Nambu, G. Los, S. Bender, B. Mroczkowski, J. Cristensen, Identification and characterization of an orally bioavailable small molecule inhibitor of c-Met kinase with cytoreductive antitumor properties in vivo, in: Proceedings of the 97th Annual Meeting of the American Association for Cancer Research, AACR, 1–5 April 2006. Washington, DC. Philadelphia (PA), p. 47. Abstract LB-273.

[27] S. Ganapaty, P. Ramalingam, C.B. Rao, Int. J. Pharmacol. Biol. 2 (2008) 13–18.

[28] Website: http://www.rcsb.org/pdb/explore.do?structureId=2wgj.

[29] H. Zhong, L. Tran, M.L. Jenna, J. Mol. Graph. Model. 28 (2009) 336–346.

[30] G. Vistoli, A. Pedretti, B. Testa, Drug Discov. Today 13 (7–8) (2008) 285–294.

[31] C.A. Lipinski, F. Lombardo, B.W. Dominy, P.J. Feeney, Adv. Drug Deliv. Rev. 46 (2001) 3.

[32] QikProp, Version 9.0, Schrodinger, LLC, New York, NY, 2010.

[33] M.C. Alley, D.A. Scudiero, P.A. Monks, M.L. Hursey, M.J. Czerwinski, D.L. Fine, B.J. Abbott, J.G. Mayo, R.H. Shoemaker, M.R. Boyd, Cancer Res. 48 (1988) 589–601.

[34] M.R. Grever, S.A. Schepartz, B.A. Chabner, Semin. Oncol. 19 (1992) 622–638.

[35] M.R. Boyd, K.D. Paull, Drug Dev. Res. 19 (1995) 91–109.